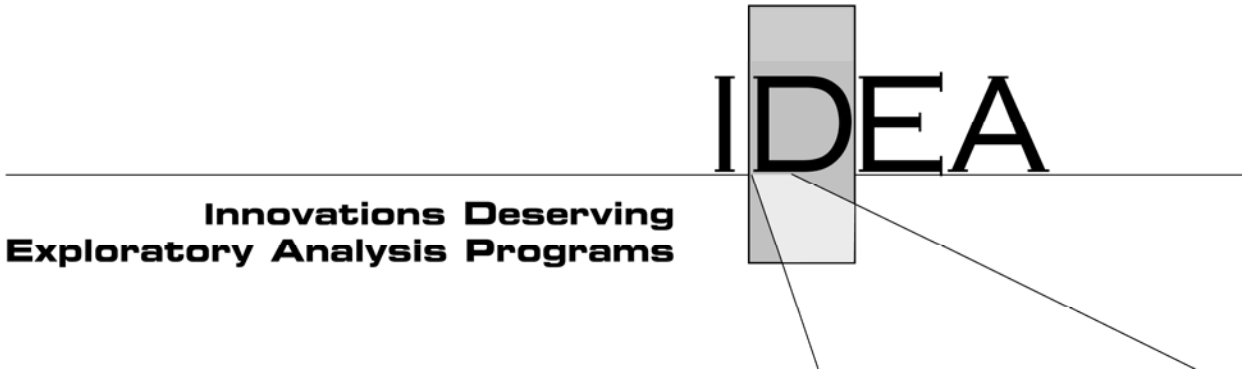

Highway IDEA Program

Long Gage-Length Interferometric Fiber-Optic Sensors for Damage Detection in Bridge Structures

Final Report for Highway IDEA Project 58

Prepared by:
Jeffrey A. Laman, and Karl M. Reichard, The Pennsylvania State University

February 2002

TRANSPORTATION RESEARCH BOARD
OF THE NATIONAL ACADEMIES

INNOVATIONS DESERVING EXPLORATORY ANALYSIS (IDEA) PROGRAMS
MANAGED BY THE TRANSPORTATION RESEARCH BOARD (TRB)

This NCHRP-IDEA investigation was completed as part of the National Cooperative Highway Research Program (NCHRP). The NCHRP-IDEA program is one of the four IDEA programs managed by the Transportation Research Board (TRB) to foster innovations in highway and intermodal surface transportation systems. The other three IDEA program areas are Transit-IDEA, which focuses on products and results for transit practice, in support of the Transit Cooperative Research Program (TCRP), Safety-IDEA, which focuses on motor carrier safety practice, in support of the Federal Motor Carrier Safety Administration and Federal Railroad Administration, and High Speed Rail-IDEA (HSR), which focuses on products and results for high speed rail practice, in support of the Federal Railroad Administration. The four IDEA program areas are integrated to promote the development and testing of nontraditional and innovative concepts, methods, and technologies for surface transportation systems.

For information on the IDEA Program contact IDEA Program, Transportation Research Board, 500 5th Street, N.W., Washington, D.C. 20001 (phone: 202/334-1461, fax: 202/334-3471, http://www.nationalacademies.org/trb/idea)

ACKNOWLEDGEMENTS

The research team thanks the oversight board (listed below) for its diligence in reviewing proposals, work plans, and progress reports during the course of the present project. Without the help of the highly qualified board this project would not have obtained the highly successful results that it did. In addition, the early work conducted by Dr. Timothy E. McDevitt during the proposal development stages of the present project are gratefully acknowledged. Graduate students Andrew J. Doller and Mike McDonagh also contributed significantly to the success of the work in developing the sensor and requisite hardware to be used for data acquisition. The resources provided by Corning Incorporated in the form of fiber samples is gratefully acknowledged. The Pennsylvania Transportation Institute support in the form of staff and student Grants-in-Aid are acknowledged as well as the Pennsylvania State University College of Engineering and the Department of Civil and Environmental Engineering for their contributions in matching equipment funding. The Pennsylvania State University Applied Research Laboratory furnished major resources and equipment to the study, without which the present project would not have been possible.

Stephen A. Cauffman
Senior Program Manager
Civil Engineering Research Foundation
Research & International Programs
Washington, D.C.

Mr. Harold Rogers, P.E.
Assistant Chief Bridge Engineer
PennDOT, Bridge Quality Assurance Division
Harrisburg, PA

Dr. Donald J. Wissuchek Jr.
Senior Research Engineer
Corning Incorporated
Corning, NY

Farhad Ansari, Ph.D.
Professor of Civil Engineering
University of Illinois at Chicago
Department of Civil Engineering and Materials
Chicago, Illinois

TABLE OF CONTENTS

EXECUTIVE SUMMARY 4

1.0 INTRODUCTION 5

1.1 PROJECT OVERVIEW 5

1.2 CURRENT STATE OF KNOWLEDGE 5

1.2.1 Long Gage-Length Sensors for Damage Detection by Modal Analysis 5

1.2.2 Fiber-Optic Sensing Systems 6

1.2.3 Previous Fiber-Optic Studies 7

1.2.4 Damage Detection 8

2.0 INVESTIGATIVE APPROACH 9

2.1 SENSING SYSTEM DESIGN 10

2.2 LABORATORY TEST STRUCTURE DESIGN AND CONSTRUCTION 13

3.0 ANALYSIS OF PHASE 2 RESULTS 19

3.1 TYPICAL RESPONSE OF OPTICAL SENSORS AND SEISMOMETERS 19

3.2 CORRELATION OF FREQUENCY RESPONSE FUNCTIONS 19

4.0 PHASE 3 DESCRIPTION AND RESULTS 22

5.0 CONCLUSIONS 27

REFERENCES 28

EXECUTIVE SUMMARY

This IDEAS project encompasses the research, development, and refining of a long gauge-length, optical fiber-based sensing system to be used for the assessment of bridge structure condition and damage detection. Two distinct detection system innovations will be derived from the current project: an optical-based strain sensing system and a long gauge-length sensor. In conjunction with the implementation of the new sensing system, damage detection techniques will be evaluated for compatibility with the proposed system.

The research program has been designed as a sequence of research and development consisting of (a) interferometric sensor design, (b) engineering of a fiber-optic-based condition assessment system, (c) development and evaluation of damage detection techniques, and (d) full-scale implementation of the system and damage detection methodologies on an existing bridge. The project consists of three phases: Phase I was the planning phase, Phase II was the laboratory study and Phase III consists of the field study. Tasks for Phases II and III were designed in conjunction with the advisory group as part of Phase I. Phase II consisted of a laboratory study on a concrete test structure and Phase III consisted of a full scale test and implementation of the system on an existing concrete bridge structure. The research program is designed to determine the relationships between the configuration of a long gauge-length fiber-optic sensing system and the ability to detect damage in large civil structures. The system has been developed and optimized in the laboratory as part of Phase II.

A study of long gauge-length, fiber-optic sensors has been conducted by the research team as part of Phase I and II. A dual-mode, long gauge-length fiber system has been developed. The interferometric system of strain measurement is used to measure dynamically induced strains along the structure. Damage was induced to the structure during the measurements. Correlation coefficients of the frequency response functions between the various damaged states and the baseline, undamaged state were calculated from the response. There is a very discernible pattern of frequency response function shifts as the damage progresses, demonstrating that the long gauge-length sensor has promise in the proposed application.

The study consists of three phases. Phase I consists of finalizing the project design in conjunction with a regional advisory group. Phase II consists of laboratory research conducted to establish the major components of the fiber-optic-based system, and develop a field system. Phase III testing was conducted at an in-service highway bridge site in Central Pennsylvania on Rte. 220 by instrumenting the existing concrete T-beam bridge (see Fig 1) with the prototype fiber-optic-based condition assessment system.

Major testing objectives and research program design were finalized during the first phase of the work. Objectives, system design, and signal processing techniques were established for both Phase II and Phase III. The research program was presented to and discussed with a regional project advisory group. The final methodology and plan of work was developed to guide Phases II and III test programs. The fundamental testing in Phase 2 optimized several features of the system, particularly as they relate to concrete bridges:

1. Evaluated adhesives for characteristics of bond, ease of application, and cure rates.
2. Evaluated fiber types for operating wavelength, polarization, and core and cladding degree and composition of doping for suitability to the proposed application.
3. Evaluated several light input sources, including lasers and light-emitting diodes.
4. Evaluated commercially available photo-detectors for sensitivity and suitability to the application.
5. Identified the influence of temperature sensitivity on the process of damage detection and condition assessment and identify methods of including a reference

Phase III consisted of testing an in-service central Pennsylvania concrete highway bridge (Fig. 1) by instrumenting (Fig. 2 and 3) the bridge with the prototype fiber-optic-based condition assessment system. This phase consisted of several tasks:

1. Evaluate and further develop the system for field applications.
2. Evaluate the durability of the system under highway conditions.
3. Evaluate the data and repeatability of the testing.
4. Evaluate the static and dynamic response measurement capabilities (Fig. 4).

This project consists of development and demonstration of the optical fiber-based instrumentation and data reduction methodologies. The proposed research will facilitate the development of diagnostic technologies that will enhance early detection of deterioration and thus may reduce the time between repair and resumption of service.

1.0 INTRODUCTION

1.1 PROJECT OVERVIEW

The need for more accurate and effective bridge condition assessment systems has become critically important, not only as the current infrastructure continues to deteriorate, but to meet higher expectations of public safety. To make the most intelligent use of resources and provide the highest possible level of public safety, accurate bridge monitoring and condition assessment techniques must be developed and implemented. Large civil structures represent a major national investment, yet most lack a monitoring system, leaving an unclear picture of the structure's physical state. Fiber-optic technology is available as a critical element in the development of a bridge monitoring system that will provide advanced information on the condition of large civil structures as well as continuous response to environmental and other events. The present research will exploit the inherent characteristics of fiber-optic cable to design, develop and implement an optical fiber for dynamic response measurement that may incorporated into such a damage detection system.

Existing sensors have relatively short gage lengths resulting in engineering information at a single point. Consequently, a network of sensors is required to accomplish a global evaluation of a large civil structure. There has been limited, but promising, success with damage detection by modal analysis using point sensors; therefore, a major objective of the present research is to develop a long gage-length optical strain sensor for detecting changes in dynamic response using pattern recognition techniques. Because sensor location is critical when using point sensors, it is expected that long gage-length sensors will be more effective in detecting changes in global dynamic response, effectively integrating the response along the length of the structure. Local effects may be lost in the integration; however, the global effects will be more pronounced and readily detected.

Three major and complimentary aspects of bridge behavior and research emerge as the focus for the goals of the present research: (1) development of a robust, long gage-length, fiber-optic sensor and sensing system; (2) development and evaluation of current and new damage detection techniques and modal analysis based on the fiber-optic data; and (3) implementation of a fiber-optic sensing and damage detection system on an existing full-scale test bridge as well as existing in-service bridges. These three goals have been pursued in cooperation with the Department of Civil and Environmental Engineering and the Applied Research Laboratory (ARL) and the Pennsylvania Transportation Institute, both major units of Penn State's Intercollege Research Programs and Facilities at the University Park campus. ARL offers a high level of fiber-optic expertise and an array of state-of-the-art equipment in support of the present research. Also, the Department of Civil and Environmental Engineering and the Pennsylvania Transportation Institute represent considerable resources.

The present project has researched, developed, and refined an innovative long gage-length, optical fiber based sensing sytem to be used for the purpose of bridge structure condition assessment and damage detection. Two distinct detection system innovations are derived from the present project: a robust optical sensing system and a long gage-length sensor. The present research is deliberately designed as a logical sequence of research and development consisting of (1) an investigation into the basic science of optical cable; (2) engineering of a fiber-optic-based condition assessment system; (3) development and evaluation of damage detection techniques; and (4) full-scale implementation of the system and damage detection methodologies on an existing Pennsylvania bridge. The program is carefully conceived to determine the relationships between the configuration of a long gage-length fiber-optic sensing system and the ability to detect damage in large civil structures. The system developed and optimized in the laboratory as preliminary research has shown the concepts to be feasible and implementable.

1.2 CURRENT STATE OF KNOWLEDGE

Much research has been conducted on optical fibers as structural sensors as well as research on modal analysis techniques. The most commonly used engineering sensors for damage detection by modal analysis are electrical, including linear variable differential transformers (LVDTs), geophones (seismometers), accelerometers, metal-foil resistance strain gages (RSGs), and piezoelectric ceramic gages. Fiber-optic sensors offer several advantages over electrical gages, which has the potential to make them valuable tools in structural evaluation, damage detection, and condition assessment. These advantages include greater sensitivity, reduced size and weight, nonconductivity, and variable gage length. Additionally, optical fibers can be used to transmit the input and output signals, eliminating the need for many electric cables and reducing the effect electrical power-line interference.

1.2.1 Long Gage-Length Sensors for Damage Detection by Modal Analysis

All of the currently existing sensors have relatively short gage lengths and can be considered as point sensors. As a result, these sensors are limited to sensing structural properties at one specific point, or a series of points if a network of sensors is used. This also includes several existing fiber-optic sensing systems, including the Fabry-Perot and Bragg Grating systems, which have been two of the most popular fiber-optic sensing systems. There has been only limited success with damage detection by modal analysis using point sensors. In general it has been difficult to detect corresponding shifts or identify patterns in resonant frequencies as a function of progressing damage in a structure using point sensors. Therefore, a major objective of the present study is to investigate the feasibility of longer gage-length sensors for detecting changes in dynamic response using pattern-recognition techniques. Because prior research has shown that sensor location is extremely important when using point sensors, it is expected that a relatively long sensor will be much more sensitive to changes in global dynamic response. The effect of a long gage-length sensor is essentially an integration of multiple sensors along the length of the structure. While certain local effects may be lost in the integration, it is anticipated that global effects, which affect the entire beam, will be more pronounced and readily detected.

1.2.2 Fiber-Optic Sensing Systems

Several types of fiber-optic sensing systems are under development. These include the Fabry-Perot, Bragg Grating, Michelson, and Mach-Zehnder systems, many of which are discussed by Jackson (1994) and Measures (1992). All fiber-optic systems operate by differing means of exploiting one basic principle: the propagation of light. Optical fibers confine and propagate light by means of complete internal reflection, accomplished at the interface of the core and cladding. If the fiber and its environment remain unchanged, the light exiting the fiber will have the same characteristics as the light entering the fiber. However, if the fiber is strained, the exiting light will have a different wavelength, intensity, or phase, depending on the system used. The resulting difference in input and output light can be translated into engineering strain, modes of vibration, and temperature change.

The two most popular fiber-optic sensing systems are the Bragg Grating sensor and the Fabry-Perot sensor. Both fibers use a circular core fiber. The Bragg Grating sensor operates by reflecting light from a finite series of gratings in the optical fiber. This grating can be applied either through physical etching of the fiber or through illuminating the fiber with ultraviolet light at a specified angle. As the etched fiber section is strained, the wavelength of the reflected light changes. Strain can be sensed by monitoring the wavelength spectrum of the reflected light. The Fabry-Perot sensor utilizes a small cavity of air along a section of the fiber. In the Fabry-Perot sensor, changes in th4e length of the air gap change the intensity and pahase of the reflected light. Fabry-Perot sensors are generally considered interferometric sensors.

Several other sensing systems are referred to as interferometric, including the Michelson and Mach-Zehnder sensors. Interferometry refers to the measurement of the interference of two light waves. A generalized interferometric strain sensor utilizes two single-mode fibers of equal length, or with a differential in length equal to a multiple of the wavelength of the light in the fibers. One fiber is attached to the element to be strained, the second fiber is isolated from that element. Light is input into both fibers at a certain phase, and changes phase over the fiber length (Masri et al., 1994). The fiber attached to the strained element will also be strained, which leads to a change in the phase of light output from the fiber. The two fibers are coupled on the output, which causes the two light waves to combine, resulting in constructive and destructive interference. This interference pattern, a light intensity varying over time, is the basis for measurement.

The fiber-optic system in the present study is interferometric; however, the underlying operation varies significantly from the generalized interferometric system discussed previously. The present interferometric system will operate with one fiber rather than two. An elliptical fiber (see Figure 1) will maintain the polarization of light within the fiber, thereby allowing discrete light waves to propagate at specific polarizations. The polarization of light is maintained by the elliptical shape of the fiber core. The glass cladding has a slightly different chemical composition than the core, which creates the core-cladding interface that internally reflects the light. The elliptical core fiber will propagate a discrete number of light modes based on the frequency of the input light. The propagation constant indicates the percentage of light propagated and not lost into the cladding. The nominal operating wavelength of an optical fiber (inversely proportional to the normalized frequency) is based on the frequency where it will propagate the first light mode. However, as the frequency of the light increases, the fiber is capable of propagating higher modes of light.

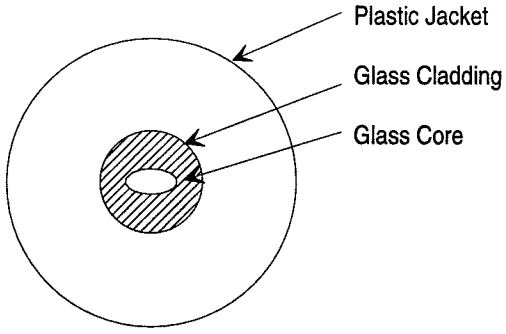

FIGURE 1 Optical fiber cross-section.

The geometric positioning of the light modes within the elliptical core fiber provides a basis for measurement. As seen in Figure 2, the second mode is discretized in the fiber cross-section to two distinct lobes of light in the core that are opposite in phase (see Dakin and Culshaw, 1988). The two out-of-phase lobes of the second mode interfere constructively and destructively
with the light of the first mode, generating a two-lobe output. As the fiber is strained, the two lobes alternate in intensity in a sinusoidal pattern. By blocking off one of the lobes, the sinusoidal variation of intensity of one of the lobes can be measured and correlated to strain, assuming that the variation of the output is between a successive peak and valley in the semi-linear output range.

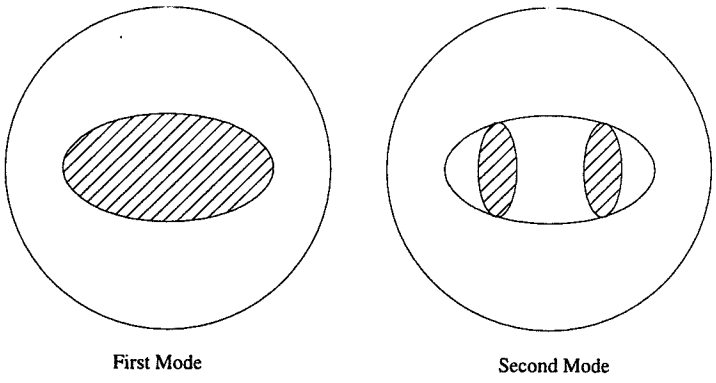

FIGURE 2. Geometric positioning of first two modes in elliptical core fiber.

1.2.3 Previous Fiber-Optic Sensor Studies

Within the past several years, research on fiber-optic sensing systems has increased as the potential for civil engineering applications was recognized. Research has confirmed the feasibility and accuracy of optical fiber sensors. Several studies have demonstrated the feasibility of various types of systems for measurement of engineering phenomena in large civil structures.

Kruschwitz et al. (1992) used small-scale reinforced concrete beams to test an extrinsic Fizeau fiber interferometric (EFFI) sensor that is very similar to the Fabry-Perot sensor, and investigated methods of embedding the sensor. Kruschwitz also attached the fiber-optic sensor to the underside of a reinforced concrete bridge and drove a calibrated truck over the bridge. The study concluded that the sensors could be embedded in and attached externally to concrete structures. Static and dynamic strain was successfully measured using the fiber-optic sensor. Nanni et al. (1991) worked with concrete cylinders to test a variable gage-length, interferometric sensor. Preliminary tests demonstrated that an assumption of a perfect bond between the concrete and the fiber was reasonable. Further testing by Nanni showed that the fiber-optic sensor can be used to provide accurate measurements of stress/strain distribution in concrete structures. Fuhr et al. (1993) built a concrete beam with embedded long gage-length, optical-fiber interferometric sensors. This study demonstrated that fiber optics can survive the concrete curing process. The study also demonstrated in a load-to-failure test that cracks in the beam that rupture the fiber can be located using optical time domain reflectometry (OTDR). OTDR measures the distance to breaks in the fiber by measuring the time of flight for short optical pulses backscattered from within the fiber. OTDR techniques present a promising means of remotely pinpointing significant cracks in structural members.

Bragg Grating and Fabry-Perot sensors have been tested by several researchers. Idriss and Kodindouma (1996) placed Bragg Grating sensors in 3-m concrete beams. Good correlation was found between the fiber-optic sensor and a foil gage. Maher et al. (1994) tested the Bragg Grating sensor on small- and large-scale reinforced concrete beams. Maher concluded that the fiber-optic sensor was effective in measuring strain in concrete. Nawy (1995) also tested a Bragg Grating fiber-optic sensor. Test specimens consisting of prestressed beams with traditional reinforcement were used. The sensor data correlated well with foil gages and were accurate for measuring stress and strain. Masri (1994) used a one-third scale model of a reinforced concrete frame joint to test a Fabry-Perot sensor. Through both static and dynamic testing, it was concluded that the fiber-optic sensor can survive concrete curing and yields accurate quantitative strain information.

Several concrete structures have already been built with embedded optical fibers. These include the Stafford Building at the University of Vermont (Huston and Fuhr, 1993a; Huston and Fuhr, 1993b; Huston et al, 1992; Robinson, 1992); a dam and powerhouse near Burlington, Vermont (Huston and Fuhr, 1993b; Robinson, 1992); and a highway bridge in Canada (Rizkalla, 1994). The Stafford building has a network of both multimode and single-mode fibers. The sensor network is intended to measure vibration, wind pressure, in-service loading, creep, temperature, and stress and strain for several years. The dam and powerhouse project in Vermont includes a fiber-optic network designed to measure vibrations caused by the turbines. The highway bridge in Canada is a precast concrete girder, pretensioned with steel and carbon fiber-reinforced plastic tendons (CFRP). Bragg Grating fiber-optic sensors are attached to the prestressing tendons at various locations for measurement of strain and temperature to monitor behavior during construction and under serviceability conditions.

The potential for fiber-optic sensors in concrete has been extensively researched; however, very few studies have been performed to examine the usefulness of optical sensors on steel structures. Huston et al. (1992) studied a multimode, long gage-length optical fiber attached to a model steel truss. The steel truss was excited by an impact loading. The vibrations were monitored using the fiber-optic sensor and accelerometers. The frequency response function from the fiber-optic sensor output was shown to compare well with the response function from an accelerometer.

1.2.4 Damage Detection

Damage detection by modal analysis requires the detection and measurement of modes and frequencies of vibration of a structure. When damage, such as cracks, broken welds, or loose bolts occurs in a structure, the stiffness is reduced and the natural frequencies are consequently altered. The actual shape, or modes of vibration could be analyzed as well with changes in the mode shapes occurring at the onset of damage in a structure. Modal analysis measures global attributes of a structure and is therefore advantageous in large civil structures where extensive networks of instrumentation are prohibitive. Most damage-detection techniques operate by imparting small amounts of energy to a local area of a structure and examining the response to that energy. Various energy forms are used, such as mechanical, radiographic, electromagnetic, magnetic, and ultrasonic (Salawu and Williams, 1995). Since only small localized portions of a structure are considered at a time, these methods can be costly and time consuming, and may lead to an incomplete assessment of a structure's state.

In contrast to traditional nondestructive testing techniques, modal analysis techniques operate on a global scale. Mechanical energy is imparted to the entire structure through various means and the response of the entire structure is analyzed. A vibrational signature is determined for the undamaged structure using two different possible parameters: resonant frequencies, and mode shapes (Mazurek and DeWolf, 1990). After an undamaged signature has been established, damage can be detected by observing changes in either of the parameters. Because of the global nature of this method, a sensor at one location is able to detect the presence of damage at a remote location by observing a change in the vibratory signature of the entire bridge.

Another advantage of modal analysis techniques is that ambient vibrations are used as the energy source. In this manner a bridge's response to traffic or wind can be continuously monitored and used to obtain a vibrational signature. The one disadvantage of ambient vibrations is that it is difficult to accurately measure the force input, and so one cannot obtain a transfer function between the inputs and outputs. However, the use of ambient vibrations is probably the most practical means of adding energy to a bridge and would be useful for an automated monitoring system.

Modal analysis techniques have been researched extensively to determine the merits of the method with only moderately successful results. Many researchers have established that damage such as cracks or fatigue in a steel superstructure can cause shifts in a structure's frequency response (Agbabian et al., 1990; Biswas et al., 1990; Mazurek and DeWolf, 1990; Paz, 1991), but those shifts are not easily detected. Mazurek and DeWolf (1990) tested modal analysis techniques on a model bridge using ambient vibrations as the energy source. The test results indicated that the concept of an automated vibration monitoring system is feasible; however, significant degradation was necessary to cause a serious effect on the dynamic response, although damage was detectable well before the onset of structural collapse. Salane and Baldwin (1990) tested both a single-span steel model bridge and a full-scale, three-span steel highway bridge.

The most prominent change in the vibratory signature occurred in the second bending mode shape, and all frequencies decreased as the testing progressed. Damping ratios also increased with progressing structural deterioration. Two full-scale bridges and a test bridge were investigated using modal analysis by Biswas et al. (1990). The study concluded that the vibratory signature was only marginally sensitive to the appearance of damage in a structure. Biswas concluded that using pattern recognition techniques on the frequency response function (FRF) appears to be more effective in detecting structural changes.

Agbabian et al. (1990) used an idealized physical bridge model made up of a grid of aluminum beams. The applied load was measured using a load cell for the calculation of a transfer function, and the response was measured with accelerometers. Agbabian arrived at several conclusions:

1. The dominant frequencies of a structure can be adequately and consistently determined using reasonable monitoring locations.
2. Changes in the frequency of a particular mode due to damage depends on the relative position of the damage in that mode, assuming only small changes in stiffness.
3. Significant damage at a location sensitive to a mode, such as an inflection point, may cause major changes in the mode shape and frequency.
4. The presence of damage or deterioration has a noticeable influence on the shape of the frequency response function.
5. It is easier to detect relatively small changes in a structure by monitoring the spacing between resonant frequencies in the FRF.
6. The input and output spectra along with the correlation between them are sensitive indicators of changes in the modal parameters.

Agbabian's work indicates the existence of a strong relationship between the position of sensor and the position of damage. By using a long gage-length sensor, as proposed in the present study, position becomes less important as the sensor measures the response of a beam over the full length.

In general, frequency shifts and changes in the mode shapes were detected when damage was applied to a structure, but the changes were not always easily detected. Biswas et al. (1990) stated that frequencies and mode shapes are only marginally sensitive to the addition of damage in a structure. Mazurek and DeWolf (1990) as well as Farrar and Doebling (1994) concluded that it was necessary to inflict serious damage on a structure before any noticeable changes in the vibratory signature occurred. One factor that is constant with all previous research is the genre of sensor. The accelerometer, as well as other sensors, were all point sensors, as they recorded structural response at one location, or at multiple discrete locations. It is this consistency in sensor type, coupled with the inconclusive results from previous work, that motivates the development of a long gage-length sensor for condition assessment.

2.0 INVESTIGATIVE APPROACH

The present project consists of three distinct but connected phases of work. The first phase of work resulted in a detailed work plan for the Phase 2 laboratory study. Following Phases 1 and 2, a Phase 3 field study will be conducted on an existing concrete bridge located in Central Pennsylvania. During Phase 1 the sensor design was finalized and the necessary equipment and supplies ordered. The project advisory group formation, approval, and meeting was an integral part of Phase 1. Near the end of Phase 1 the research team met with the advisory group and discussed the research program and the proposed work plan. Suggestions and comments received from the project advisory group were incorporated into the final research work plan to the greatest extent possible within the original scope and budget. The final work plan was submitted to the NCHRP IDEAS project manager. Below is a synopsis of Phase 2 work completed.

Phase 2 encompasses the laboratory development of optical sensors, construction of a concrete scaled bridge model, and testing of the sensors for use in damage detection. The optical sensors and the laboratory specimen and test program have been designed as described in the Phase 2 Work Plan and are presented here in Figures 3 through 18. Phase 2 is complete with both the small test beam (f'_c = 3750 psi) and the larger concrete test structure built and cast (f'_c = 4900 psi), and all sensors and data acquisition equipment design and development complete. Testing of the sensors in the small beam and the larger test structure was successful with response records collected using both the optical fiber sensors embedded in the concrete beam and test structure and seismometers.

The project team built and constructed the small 7'- 0" long by 4" deep by 9¼" wide test beam to ensure that the concept for the optical fiber sensors was functional before building and casting the larger test structure. Epoxy techniques, fiber splice protection, fiber de-coupling, and fiber exit details were tested for survivability of construction on the small test beam. Figure 11 depicts each of these features for the small concrete test beam. The optical fiber sensors

embedded in the small test beam functioned as designed with measurement of strain along the coupled length of the fiber sensor.

Following the construction and evaluation of the small test beam, the larger test structure was built and cast as shown in Figures 15 and 16. Eight fiber sensors were embedded in this test structure with 6 attached to reinforcing bars, 1 embedded in the plain concrete, and 1 retrofitted in a cut groove in anticipation of the Phase 3 installation. In addition to the test structure, a drop weight device was designed and constructed as shown in Figure 21 to serve as controlled loading for the data collection phase of the project.

The electronics required for the fiber sensor were designed and constructed for the project as well. An appropriate laser light source has been obtained and an assembly constructed to focus the light into the fiber end as shown in Figure 6. The photo detector has been designed and built including optics to focus exiting light, a photo diode, and an amplifier for the photo diode signal as shown in Figure 10. The fundamental laboratory testing in Phase 2 optimized several features of the proposed system as they relate to both steel and concrete structures:

1. Evaluated adhesives for characteristics of bond, ease of application, and cure rates as well as reaction with fiber jacket.
2. Evaluated commercially available fiber types specified with different combinations of cladding diameter, jacket diameter, operating wavelength, polarization, and core and cladding degree and composition of doping for suitability to the proposed application.
3. Evaluated laser light input sources in terms of wavelength, type, durability, stability, and resulting signal quality.
4. Evaluated commercially available photo detectors for sensitivity and suitability to the application.
5. Identified the influence of temperature sensitivity on the process of dynamic damage detection and condition assessment.

2.1 SENSING SYSTEM DESIGN AND CONSTRUCTION

The sensing system consists of several components that are shown in Figure 3 below. The sensing section of optical fiber is an elliptical core polarization maintaining fiber with a core index of refraction of 1.4824, a cladding index of refraction of 1.4504, a cladding diameter of 80 microns (± 3 microns), a jacket diameter of 200 microns (± 15 microns), and ellipse radius of 1.25 μm x 2.5 μm . The nominal operating wavelength is 820 nm, propagating a single mode in the 760 nm to 900 nm wavelength range. It has a Germanium doped silica core with Fluorine doped silica cladding. The fiber temperature sensitivity is dominated by the silica outer jacket which has a thermal expansion coefficient of $5x10^{-7}$ per °C temperature change. The non-

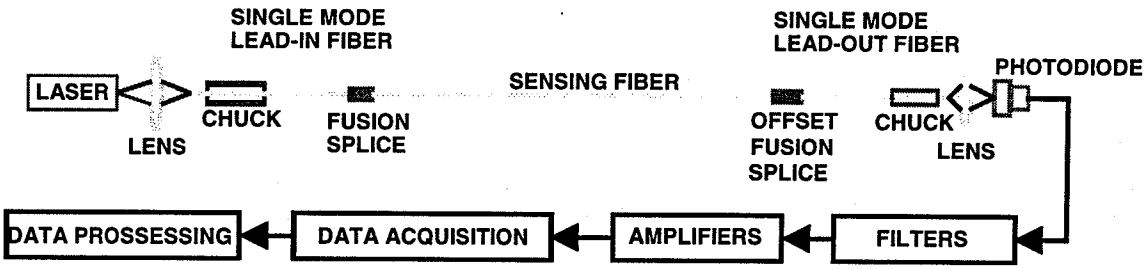

FIGURE 3. Sensing System Configuration.

sensing lead-in and lead-out fiber is a single mode, 633 nm, also with a Germanium doped silica core with Fluorine doped silica cladding. A coupler is used to focus the light into the optical fiber. Practically, the coupler is a microscope objective mounted on an adjustable base. The coupler can be rotated so that the laser light is projecting through the microscope lens and directly into the end of the fiber. The optical fiber is held in place by a fiber chuck that grasps the fiber and fits into a mount on the coupler. A high-speed (-3 dB) modulation of 50 MHz photodiode is used that converts light intensity into voltage and passes the voltage to a filter and amplifier.

The amplifier (see Figure 4) is a reverse biased amplifier intended to decrease noise in the circuit and provide stability. The amplified voltage is passed to a high voltage isolated analog input data acquisition module. R1 and C1 determine the 3dB cut off point of the low pass filter (2 kHz) $f = 1/(2\pi R C)$. R2 and C1 determine the 3dB cut off point of the high pass filter (1 Hz). The DC is actually passed through but is not amplified where as the AC is amplified. R2 and R3 determine the gain of that stage (Currently 5) R3/R4 + 1. R4 and R5 determine the gain of that stage (Currently 20). The signal is then sent to a data acquisition board through an input card at 16 bit analog to digital conversion. A

commercially available data acquisition and analysis software package was used to record the data and to perform the necessary statistical functions, digital filtering, spectral analysis, fast Fourier transform (FFT) analysis, and logical operations.

Two lasers were used in the laboratory testing for Phase 2. A larger, bench-top type standard helium-neon laser (see Figure 5), with an operating wavelength of 633 nm and output power of 5 mW with transverse electrical-magnetic linear polarization was used as well as a red laser diode (see Figure 5 and 6) with an operating wavelength of 635 nm. The laser diode was chosen because it has a stable light output of 3 mW with linear polarization and it is of a size that is suitable for the field testing of Phase 3. A coupler is used to focus the light from the laser into the optical fiber. The coupler is essentially a microscope mounted on an adjustable base that can be rotated so that the laser light projects through the microscope lens and directly into the end of the fiber.

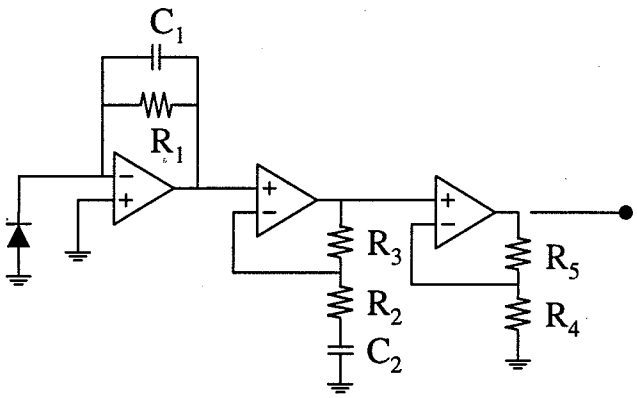

FIGURE 4. Schematic of Amplifier.

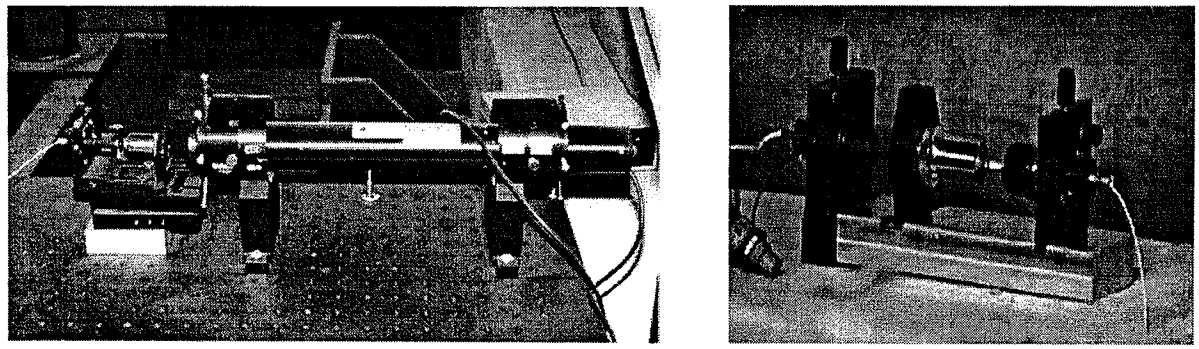

FIGURE 5 Helium-Neon Laser (left) and Laser Diode Device (right)

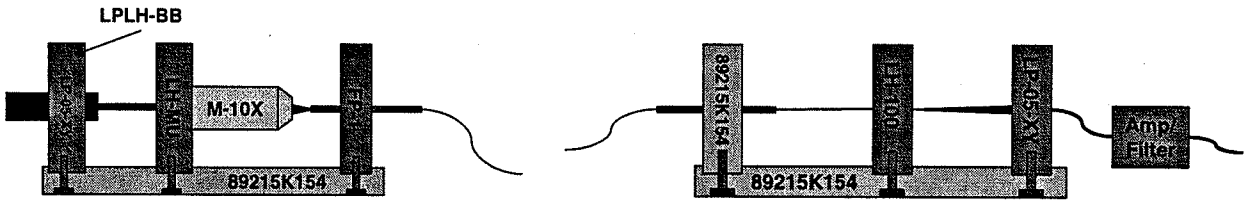

a) Laser Input

b) Signal Output

FIGURE 6 Construction and Configuration of Laser Light Input Jig and Signal Output Jig.

An alternative method investigated for monitoring the output of one light mode consists of a lens placed several centimeters from the end of the fiber. This causes the two lobes of light to separate, allowing one lobe to be identified and blocked (see Figure 7). The lens then focuses the remaining light mode on the photodetector. This method requires precise alignment of the fiber end with the lens, the lens shield, and the photodetector, making this method somewhat less practical for field applications; however, the fusion splice is not required. Tests in the laboratory demonstrated that this method is feasible for field applications and, due to the low cost, will be used for the Phase 3 testing.

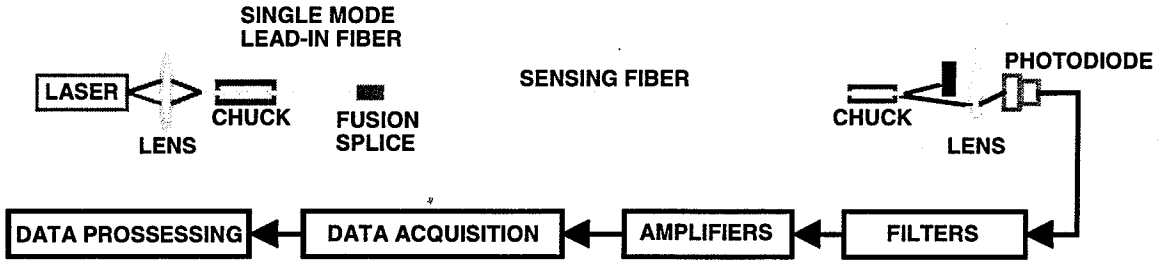

FIGURE 7 Alternate Optical Sensing System

The sensor construction involved cleaving the ends (see Figure 8) of the MM and SM fibers in preparation for the fusion splice (see Figure 8). The offset splice presented a significant challenge, however, with time the method was perfected. When the fusion splice had been accomplished, it was encased in a steel case as shown in Figure 9. This prevented damage to the relatively fragile link in the sensor system during the concrete placing stage.

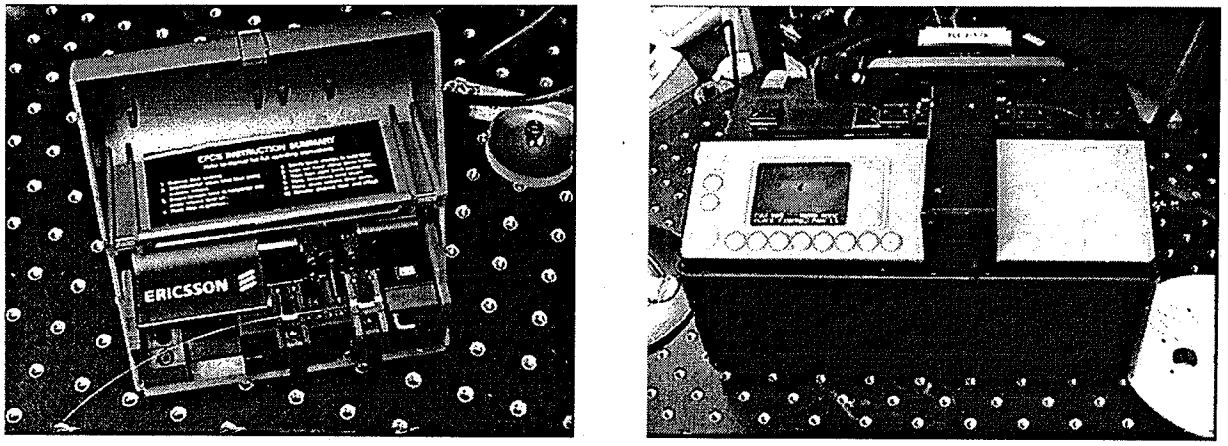

FIGURE 8 Ericsson Cleaving Device (left) and Fiber Splicing Device (right).

In preparation for Phase 3 field testing, the laser diode light input and photo diode output (see Figure 10) was ruggedized and placed in aluminum protective containers. These containers also prevented any noise generating light from contaminating the signal during controlled testing in the laboratory as well as protecting the input and output from dust.

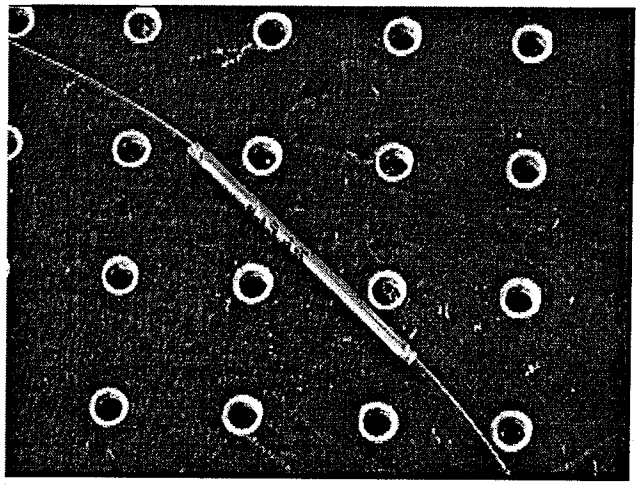

Figure 9. Protection of Offset Fusion Splice.

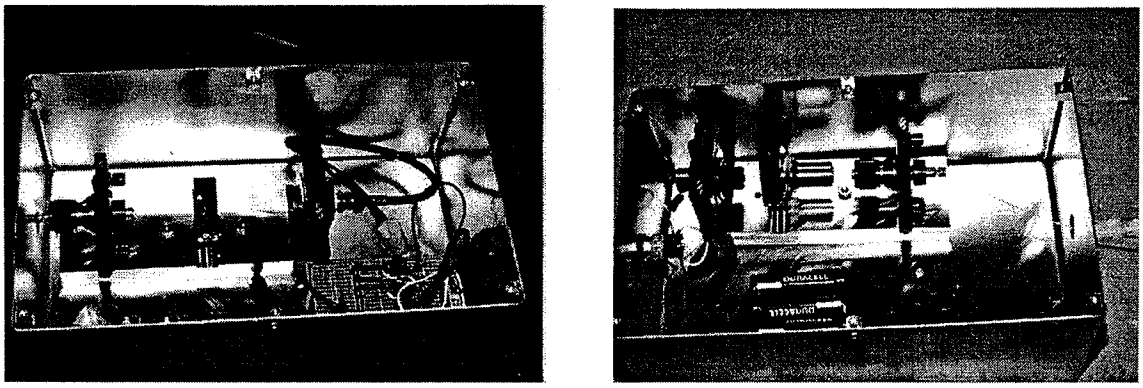

FIGURE 10 Ruggedization of the Laser Diode Input (left) and Photo Diode Output (right).

2.2 LABORATORY TEST STRUCTURE DESIGN AND CONSTRUCTION

Phase 2 laboratory testing of the sensing system involved the construction of two test structures for evaluation. The first test structure was constructed as a preliminary specimen to ensure that the fiber attachment, entrance, and exit would function properly (see Figure 11). The preliminary test beam measured 4" deep by 9¼" wide by 7'- 0" long (95 mm deep by 235 mm wide by 2130 mm long) and contained two (2) #3 reinforcing bars. Each of the two reinforcing bars were instrumented with sensing fibers for preliminary testing. The preliminary tests of (1) epoxy of fiber to reinforcing bar; (2) protection of the fusion splice; (3) decoupling for the fiber in the formwork; and (4) placement and curing of concrete were successfully completed and the construction of the large laboratory concrete test structure proceeded.

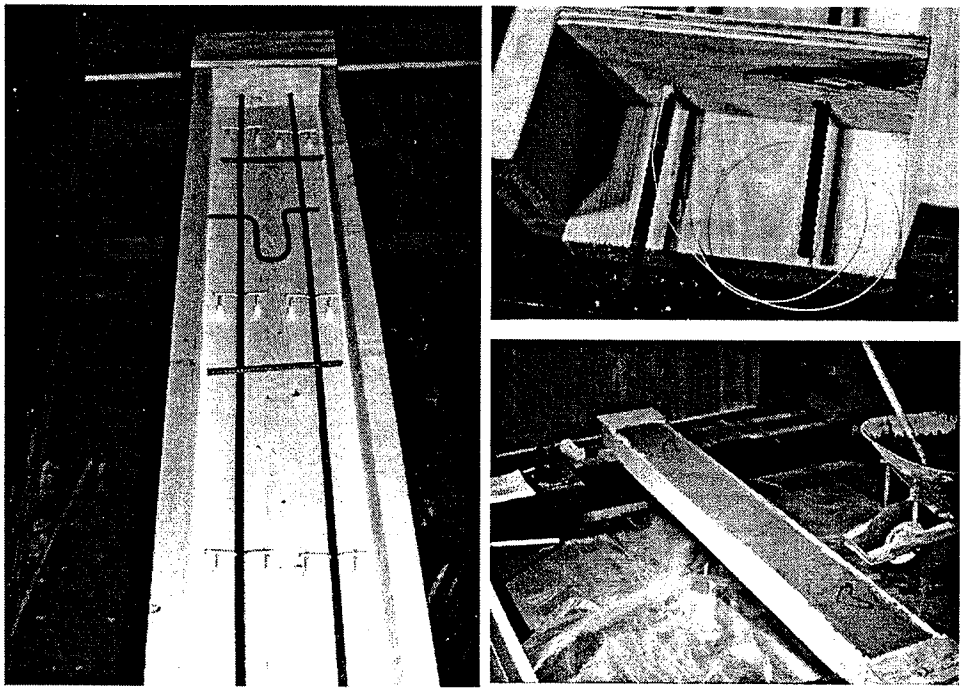

FIGURE 11 Small Test Beam – Rebar Placement (left), Fiber Entrance and Exit (upper right) and Cast Beam (lower right).

The large laboratory concrete test structure design and sensor location was based on the long-gage-length characteristics of the optical sensor. The schematic design of the test structure is shown in Figure 12, indicating overall dimensions and rebar placement. The sensor location design is based on the recognition of the various mode shapes of the test structure and the integrative properties of the sensor. As shown in Figure 13, the sensor must be strategically placed to properly respond to particular modes of vibration. The seven sensors were, therefore, placed so as to respond to

the several identifiable modes of the structure as shown in Figure 14. Sensor A is placed to respond primarily to the 1st and 3rd mode and exhibit very little response to any other modes. Sensor B is placed to respond primarily to the 1st and 2nd mode; Sensor C to the 1st, 2nd and 5th modes; Sensor D to the 1st, 3rd, and 5th modes.

The forming and placing of optical sensors proceeded as shown in Figures 15 through 18. Figure 15 is an overall view of the completed forming, rebar placing, and sensor installation. The sensors were attached to the rebar with epoxy as seen in Figure 16, creating the sensing section and gage-length for the optical sensor. Where the multimode fiber continued adjacent to the rebar beyond the gage-length, it was necessary to isolate the fiber from the rebar to decouple the fiber from the reinforcing bar and to prevent inadvertent strains. This was accomplished by placing the multimode fiber inside a small diameter aluminum section of medical tubing (see Figure 16) from the end of the gage length to the exit point of the fiber from the test structure (see Figure 17).

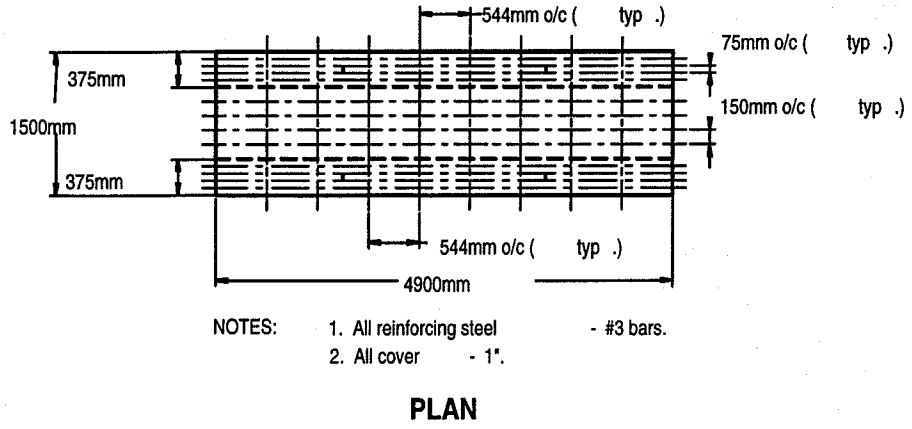

FIGURE 12 Schematic Drawing of Laboratory Concrete Test Structure.

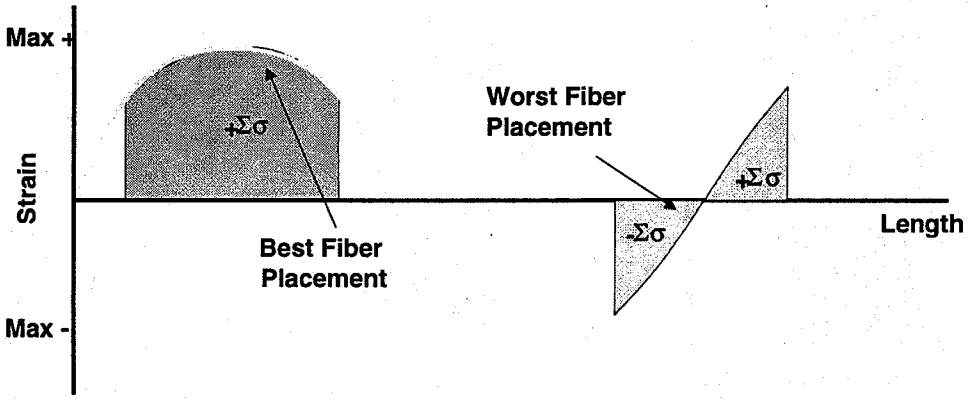

FIGURE 13 Optimal Sensor Placement.

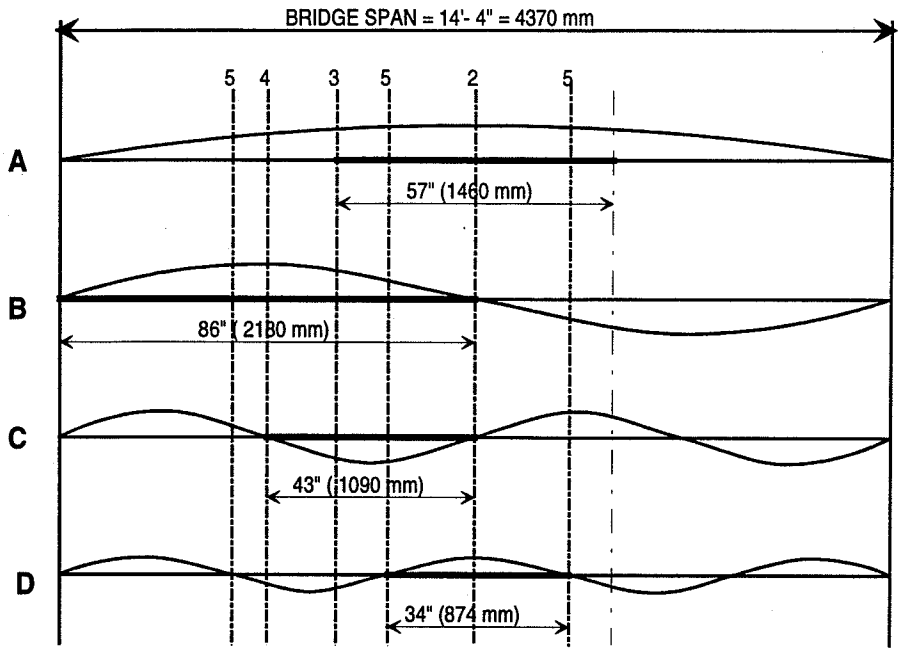

SENSOR GAGE LENGTHS AND TYPE

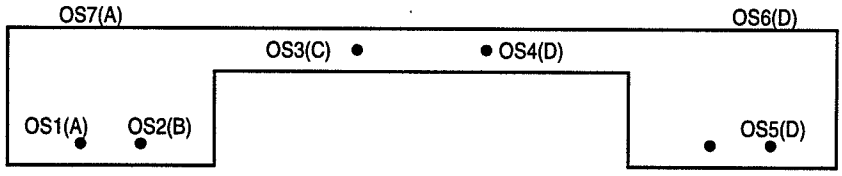

SENSOR TYPE LOCATIONS (END VIEW)

FIGURE 14 Schematic Drawing of Laboratory Concrete Test Structure.

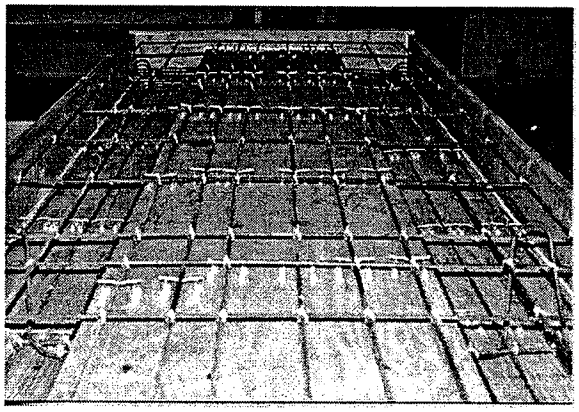

FIGURE 15 Forming of the Laboratory Concrete Test Structure and Placement of Rebar.

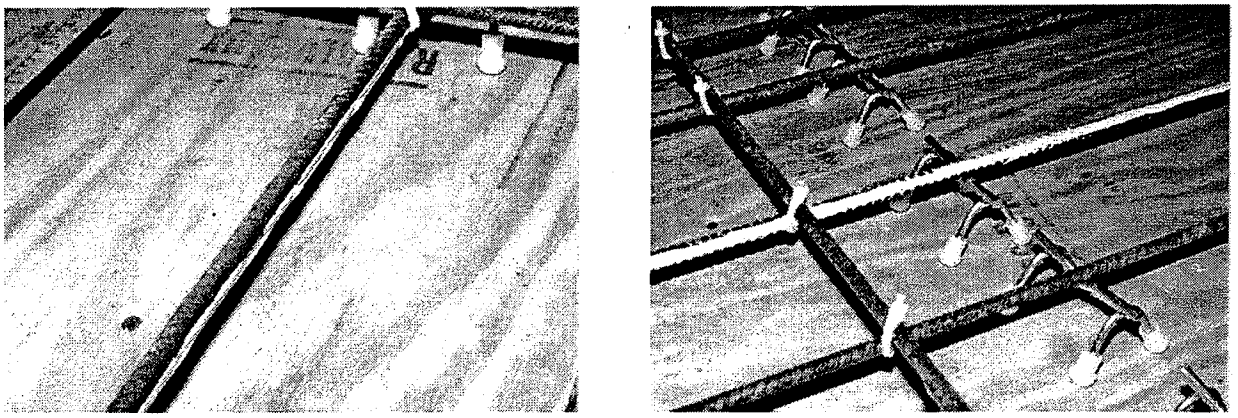

a) Isolation of Sensing Fiber in Aluminum Tube.

b) Epoxy of Sensing Fiber Directly to Rebar.

FIGURE 16. Placement of Optical Sensors Attached to the Rebar.

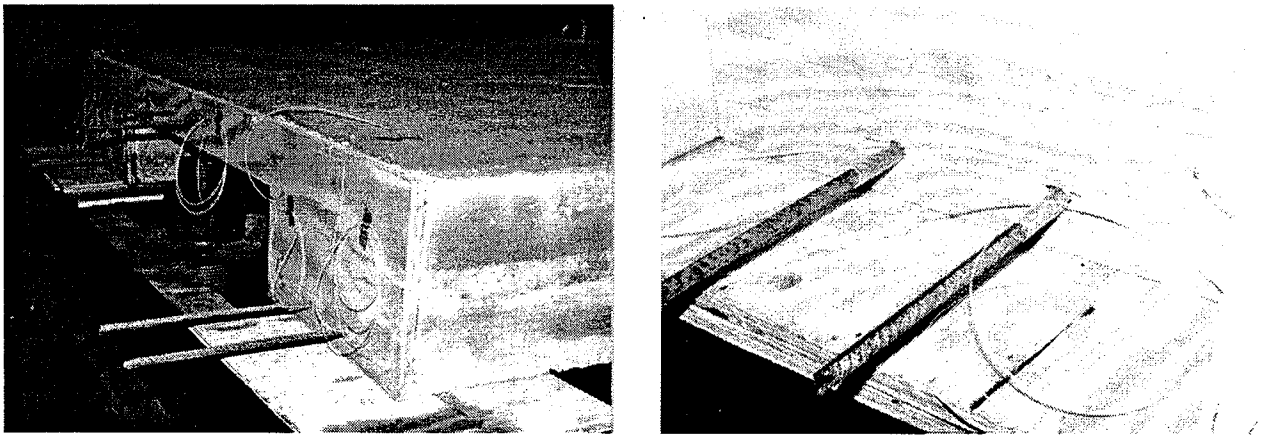

FIGURE 17 Optical Fiber Exit and Entrance to the Test Structure.

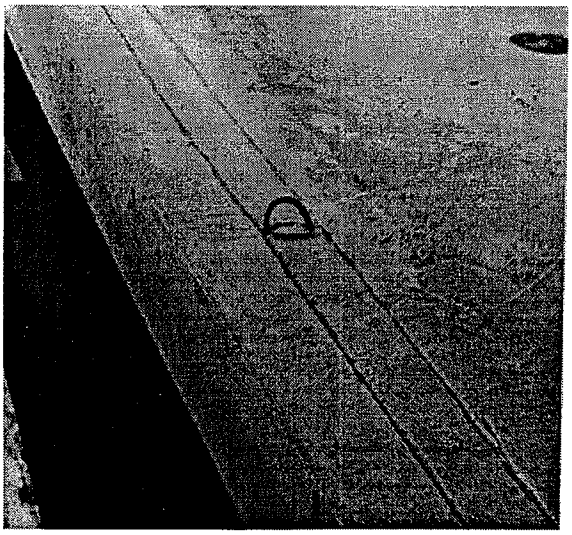

FIGURE 18. Retrofit Saw-cut Groove for Placement of the Optical Fiber Sensor.

The data sets collected for the laboratory testing consisted of 3 stages. The sages were: 1) undamaged state; 2) partially damaged state; and 3) fully damaged state. The magnitude of the damage is presented in Figure 19; the damage being a saw cut made in the locations shown directly through the depth of the concrete structure and corresponding rebar at each edge of the test structure at midspan. The excitation for each of the experiments was an impact of known and consistent energy on the test structure surface at 4 different locations using two different energy levels. Locations of impacts and type are shown in Figure 20. The impact device is shown in Figure 21, which is a drop weight device that can be adjusted by height and/or by weight to alter the excitation energy input.

The data sets were taken as shown in Tables 1 through 3 and consist of nine sets for each impact location, taking data from two optical sensors and two vertical seismometers during each set. This scheme resulted in 396 sets of 4 data channels, or 1584 channels of data between the undamaged, partially damaged, and fully damaged states.

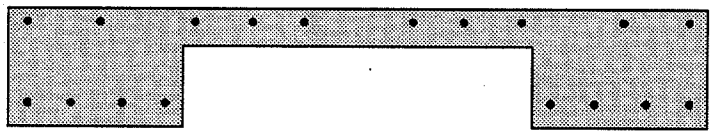

a) Undamaged Cross-Section.

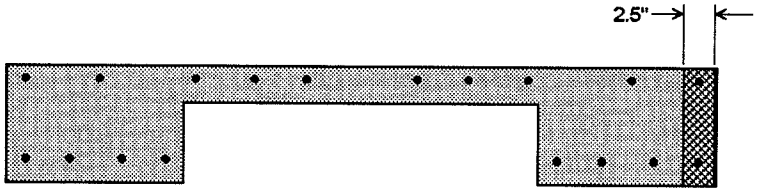

b) Partially Damaged Cross-Section.

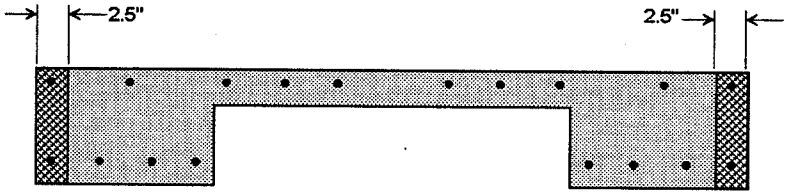

c) Fully Damaged Cross-Section.

FIGURE 19 Progressive Damage to Cross-Section at Midspan of Test Structure.

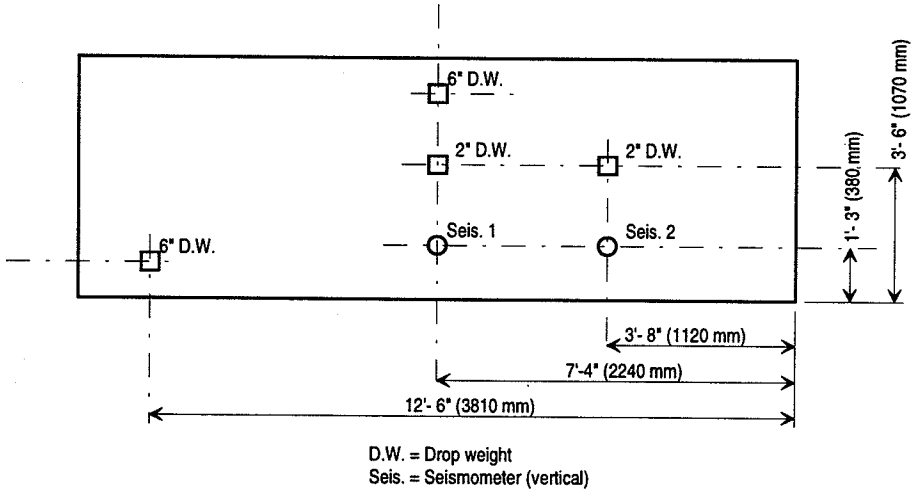

FIGURE 20 Plan View of Concrete Test Structure Location Seismometers and Impacts.

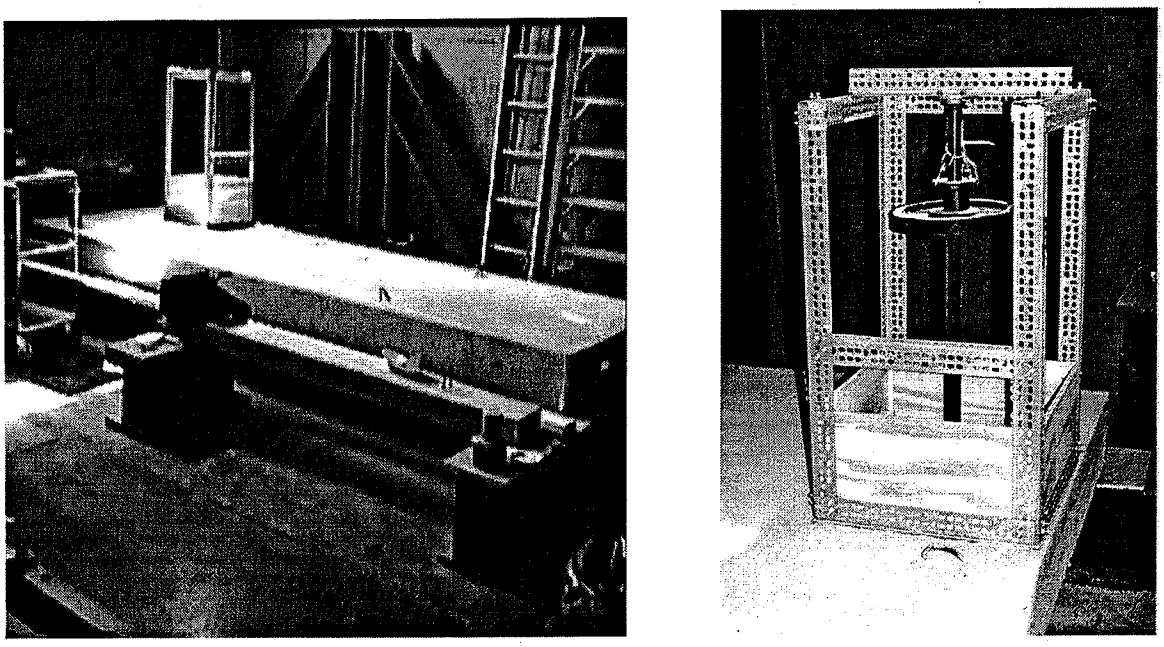

FIGURE 21 Position of Drop Weight (left) and Drop Weight (right).

Table 1. Undamaged - Active Sensors and Test Description with File Designations.

	Test Description				
Active Sensor	2" Drop, ½ pt.	2" Drop, ¼ pt.	6" Drop, ½ pt.	6" Drop, ¼ pt.	Noise Test
OS4 + OS3	21102.*	21103.*	--	215001.*	--
OS4 + OS5	32012.*	32013.*	32011.*	32014.*	321*NOS
OS4 + OS6	37001.*	37002.*	37004.*	37003.*	37NOS1,2,3,4
OS4 + OS7	32001.*	32002.*	32004.*	32003.*	320*NOS

Table 2. Partial Damage - Active Sensors and Test Description with File Designations.

	Test Description				
Active Sensor	2" Drop, ½ pt.	2" Drop, ¼ pt.	6" Drop, ½ pt.	6" Drop, ¼ pt.	Noise
OS4 + OS3	320001.*	320002.*	320004.*	320003.*	320NOS1,2,3,4
OS4 + OS5	310001.*	310002.*	310004.*	310003.*	310NOS1,2,3,4
OS4 + OS6	39002.*	39003.*	39001.*	39004.*	39NOS1,2,3,4
OS4 + OS7	312002.*	312003.*	312001.*	312004.*	328NO11,2,3,4

Table 3. Full Damage - Active Sensors and Test Description with File Designations.

	Test Description				
Active Sensor	2" Drop, ½ pt.	2" Drop, ¼ pt.	6" Drop, ½ pt.	6" Drop, ¼ pt.	Noise
OS4 + OS3	328001.*	328002.*	328003.*	328004.*	328NOS1,2,3,4
OS4 + OS5	330001.*	330002.*	330003.*	330004.*	330NO1,2,3,4
OS4 + OS6	Sensor OS6 Damaged				
OS4 + OS7	328011.*	328012.*	328013.*	328014.*	328NO11,2,3,4

3.0 ANALYSIS OF PHASE 2 RESULTS

3.1 TYPICAL RESPONSE OF OPTICAL SENSORS AND SEISMOMETERS

Sample time-history response functions are presented in Figures 22 through Figure 24 for optical sensor 4 (OS4), optical sensor 5 (OS5), and seismometer 1 for an impact at the ¼ point of the test structure. As a means of evaluating the response, frequency response functions (FRF) were developed for each time-history record. The FRF of the OS5 sensor time-history presented in Figure 23 is found in Figure 25 for no damage and full damage. Correspondingly, the FRF of the seismometer 1 time-history shown in Figure 24 is presented in Figure 26. It can be observed that a significant increase in power of the second frequency occurs for the OS5, while that frequency is already present with little change in power for the seismometer.

3.2 Correlation of Frequency Response Functions

As a means of identifying differences in response spectra other than visually identifying trends and differences, correlation coefficients were computed for the frequency response functions. A correlation coefficient is a measure for comparison of two arrays of data and describes the relationship between them by a value between -1 and +1. A zero value indicates that there is no relationship or correlation between the two arrays of data, and the data are said to be independent. A +1 and -1 value indicate that there is perfect correlation or anti-correlation, respectively, between the sets of data. For two arrays of data X and Y, the equation for the correlation coefficient $\rho_{x,y}$ is

$$\rho_{x,y} = \frac{Cov(X,Y)}{\sigma_x \cdot \sigma_y}$$

where

$$Cov(X,Y) = \frac{1}{n}\sum_{i=1}^{n}(x_i - \mu_x)(y_i - \mu_y)$$

and μ_x, μ_y are the mean values of the arrays and σ_x, σ_y are the standard deviations.

For each case, data were taken in several sets as described previously at each stage of damage. Correlation coefficients between data from the impacts before the structure was damaged and from impacts at each stage of damage were computed. The average of these coefficients was computed, resulting in one average correlation coefficient relating the undamaged state with a stage of damage. The standard deviation of the set of correlation coefficients was also computed. Finally, the average correlation coefficient and standard deviation were computed, comparing each stage of damage with the undamaged state. See Figure 27 for a diagram of the general correlation coefficient analysis.

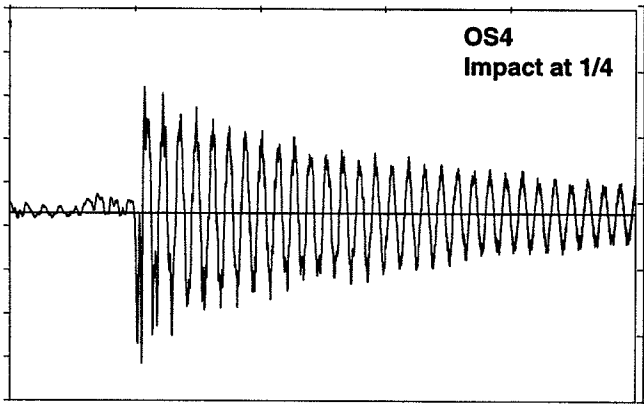

FIGURE 22 Time-History of Optical Sensor OS4.

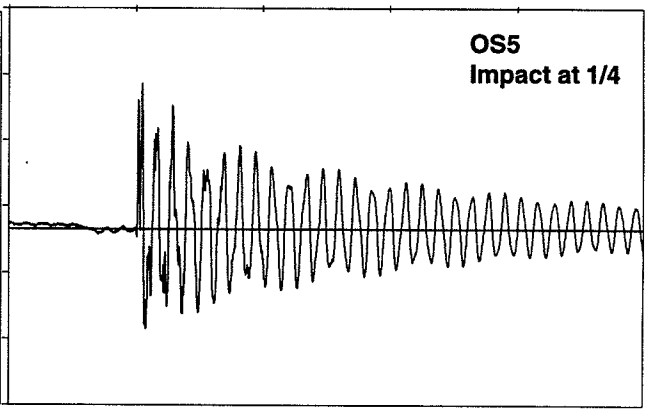

FIGURE 23 Time-History of Optical Sensor OS5.

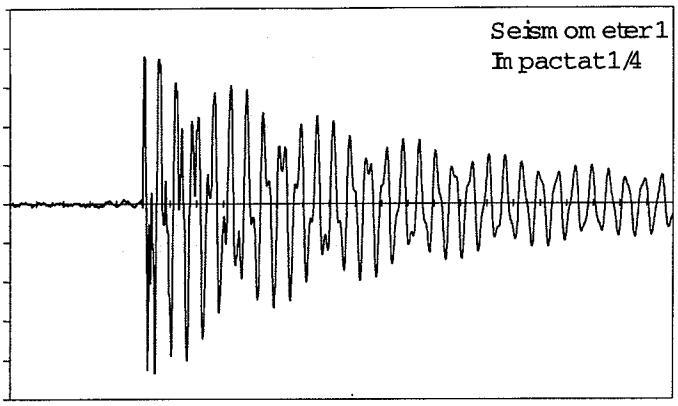

FIGURE 24 Typical Dynamic Time-History Response of Optical Seismometer 1.

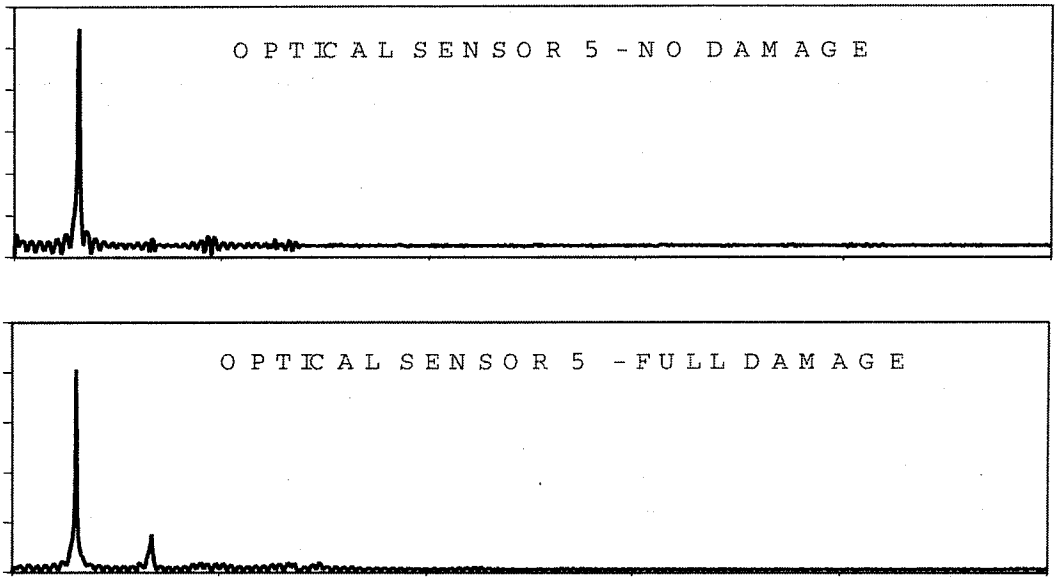

FIGURE 25 Power Spectral Density Functions of Typical Optical Sensor Time Histories.

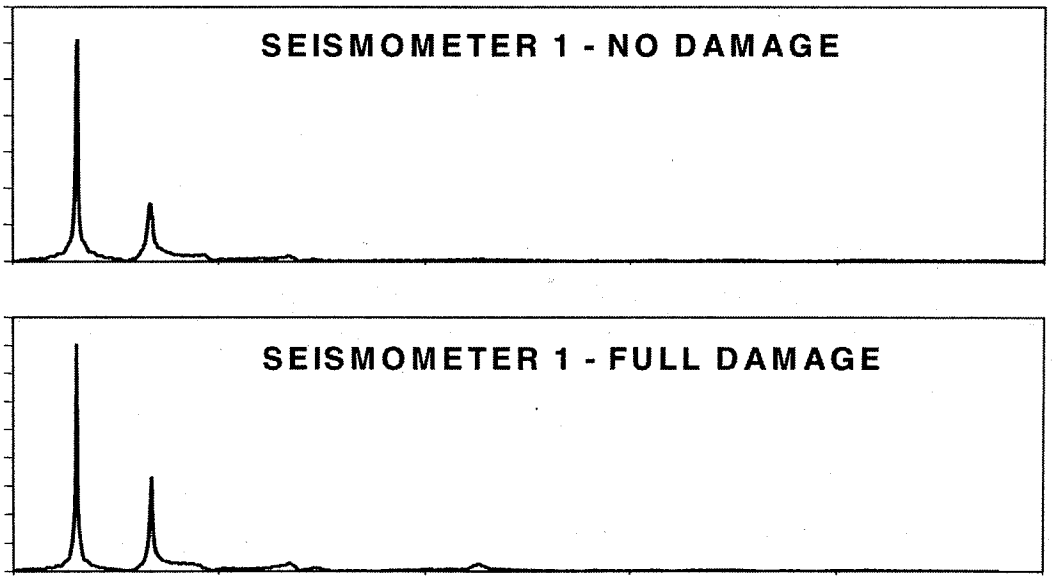

FIGURE 26 Power Spectral Density Functions of Typical Seismometer Time Histories.

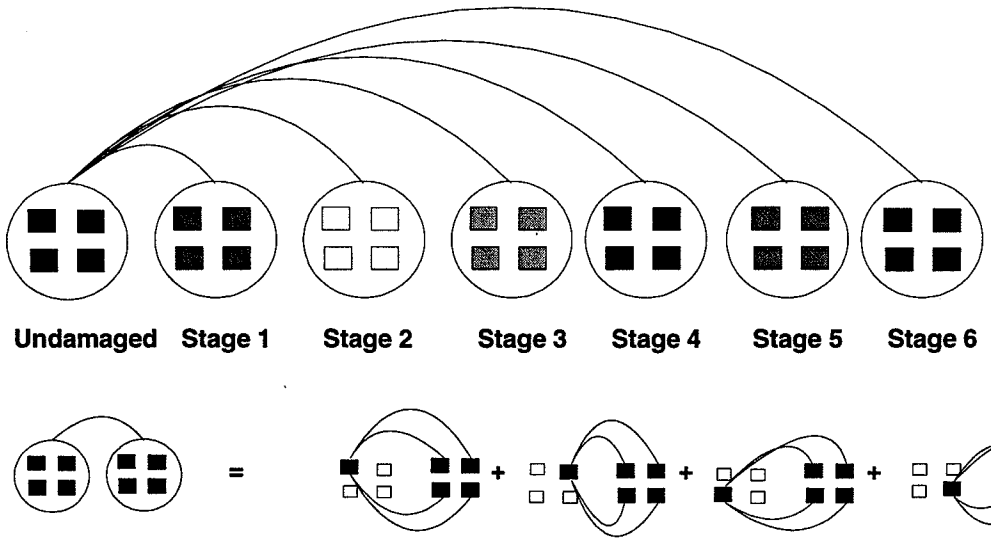

FIGURE 27 Correlation Procedure Between Stages of Damage and Correlation of Individual Tests.

Each test shown in Tables 1, 2, and 3 consisted of 9 trials. Each trial was processed to determine the FRF and then each FRF was correlated with every other FRF. The results of a sample correlation for OS3 between the undamaged stage and the partially damaged, conducted as described in Figure 27, is presented in Table 4. This procedure resulted in 48 tables similar to Table 4 which were developed to evaluate each of the Table 1, 2, and 3 tests for 2" drop, 6" drop at the ½ and ¼ point locations in the undamaged, partially damaged, and fully damaged stages. Tables 5 and 6 present the averages of the OS3 sample correlation procedure for the case of undamaged to partially damaged and undamaged to fully damaged respectively.

Table 4 Optical Sensor OS3- Spectral Density Correlation Factors between Partially Damaged vs Undamaged, 6" Drop at ¼ Point

	1 undam	2 undam	3 undam	4 undam	5 undam	6 undam	7 undam	8 undam	9 undam	Average
1 p. dam	0.074	0.110	0.082	0.096	0.143	0.095	0.110	0.132	0.069	0.101
2 p. dam	0.112	0.130	0.075	0.130	0.180	0.128	0.139	0.167	0.092	0.128
3 p. dam	0.113	0.165	0.152	0.124	0.141	0.117	0.160	0.167	0.137	0.142
4 p. dam	0.113	0.165	0.152	0.124	0.141	0.117	0.160	0.167	0.137	0.142
5 p. dam	0.084	0.109	0.026	0.073	0.130	0.080	0.116	0.137	0.062	0.091
6 p. dam	0.061	0.094	0.102	0.033	-0.053	0.009	0.102	0.084	0.130	0.062
7 p. dam	0.109	0.140	0.085	0.116	0.163	0.116	0.144	0.158	0.104	0.126
8 p. dam	0.112	0.157	0.208	0.099	0.018	0.079	0.149	0.131	0.188	0.127
9 p. dam	0.136	0.162	0.104	0.138	0.206	0.168	0.157	0.189	0.118	0.153
Average	0.097	0.134	0.110	0.099	0.108	0.093	0.135	0.143	0.115	0.112

Table 5 Optical Sensor OS3 Average Spectral Density Correlation Factors Between Undamaged and (1) Partially Damaged; (2) Full Damage, 6" Drop at ¼ Point.

	OS3	OS4	OS5	OS6	OS7
Undamaged → part. damage	0.112	0.876	0.630	0.735	0.895
Undamaged → full damage	0.252	0.174	0.215	--	0.118

Table 5 Average Spectral Density Correlation Factors Between Undamaged and (1) Partially Damaged; (2) Full Damage, 2" Drop at ¼ Point.

	OS3	OS4	OS5	OS6	OS7
Undamaged → part. damage	0.292	0.982	0.850	0.953	0.952
Undamaged → full damage	0.712	0.712	0.774	--	0.943

Figures 27 a) and 27 b) graphically illustrate the decay of the FRF correlations with the no-damage state for OS3, OS4, OS5, OS6 and OS7. All optical sensors except OS3 exhibited a decay in the FRF correlation coefficients for both the 2" drop and the 6" drop at the ¼ point. Similar results were obtained for the 2" drop and 6" drop at the ½ point. It can be observed that the 6" drop FRF correlation coefficient decay is more pronounced indicating that higher energy input levels are required to properly excite all modes and observe the trend.

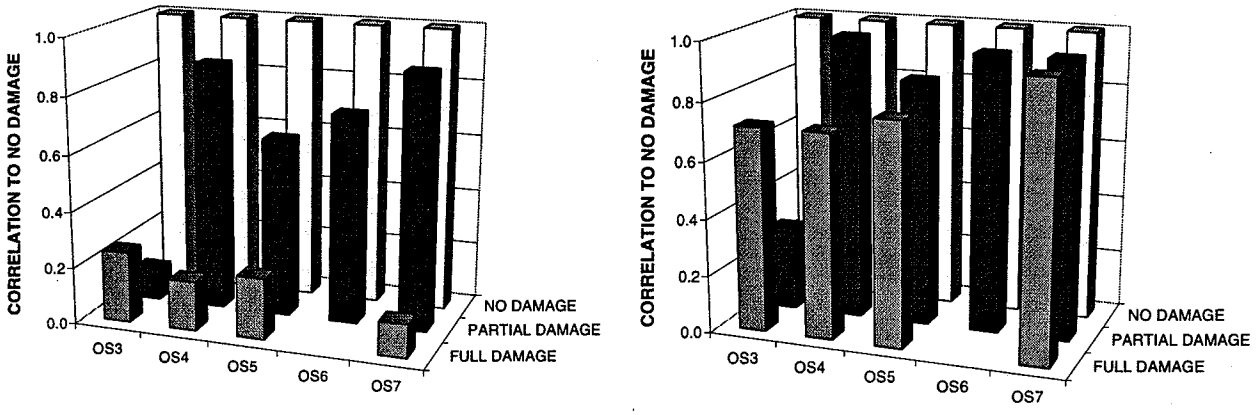

a) 6" Drop at ¼ Point.

b) 2" Drop at ¼ Point.

FIGURE 27 Bar Graph of Correlation Decay with Damage.

Based on the previously discussed positive results obtained during Phase 2 of the study, Phase 3 of the study was undertaken. Phase 3 applied the same interferometric sensor design used in Phase 2 to a full-scale bridge structure owned by the Pennsylvania Department of Transportation (PennDOT).

4.0 PHASE 3 DESCRIPTION AND RESULTS

Phase 3 consisted of testing an in-service, concrete, T-beam bridge by instrumenting the existing structure near the bottom of two stems with the prototype, interferometric fiber-optic-based sensors. As Phase 3 consisted of instrumenting an actual bridge structure, PennDOT provided locations of 5 bridges for consideration. These bridges were visited by the project team and inspected for the project criteria. Bridge 14-0220-0350-0690 near Unionville, PA (see Figure 28) was selected for Phase 3 of the project. The bridge experiences approximately a 1000 average daily truck traffic, allowing adequate loading for the collection of response due to normal traffic. Elevation photographs of the bridge are shown in Figure 29 and drawings of the bridge partial plan, half elevation, beam and parapet, and half section are shown in Figure 30. The bridge is a 45'- 0" span concrete T-beam structure constructed in 1925 with 8 beams.

Phase 3 consisted of several tasks:

1. Installation of the optical sensors.
2. Evaluate and further develop the durability of the system for field applications.
3. Evaluate and further develop the system for field applications.
4. Evaluate the quality of data and repeatability of the testing.
5. Evaluate the static and dynamic response measurement capabilities.

Installation of the optical sensors required making saw-cut grooves in the concrete and epoxying the sensor into place over the desired gauge length. The saw-cut was completed as shown in Figures 31 and 32. An approximately 45 degree, $^{3}/_{16}$ inch groove was made in the second and third girders from the West with a standard concrete cutting blade and hand-held saw. The optical-fiber sensor was then laid into the saw-cut groove and epoxy was injected around the fiber. The epoxy was allowed to set for 24 hours before the testing was initiated. Figure 32 shows the completed optical fiber installation and the instrumentation setup for the field test conducted on the in-service bridge structure.

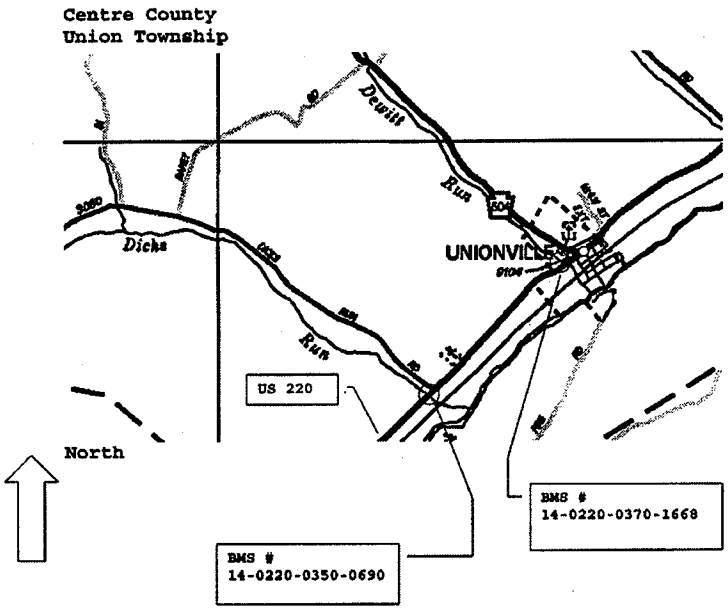

FIGURE 28 PennDOT BMS Map Locating Bridge 14-0220-0350-0690.

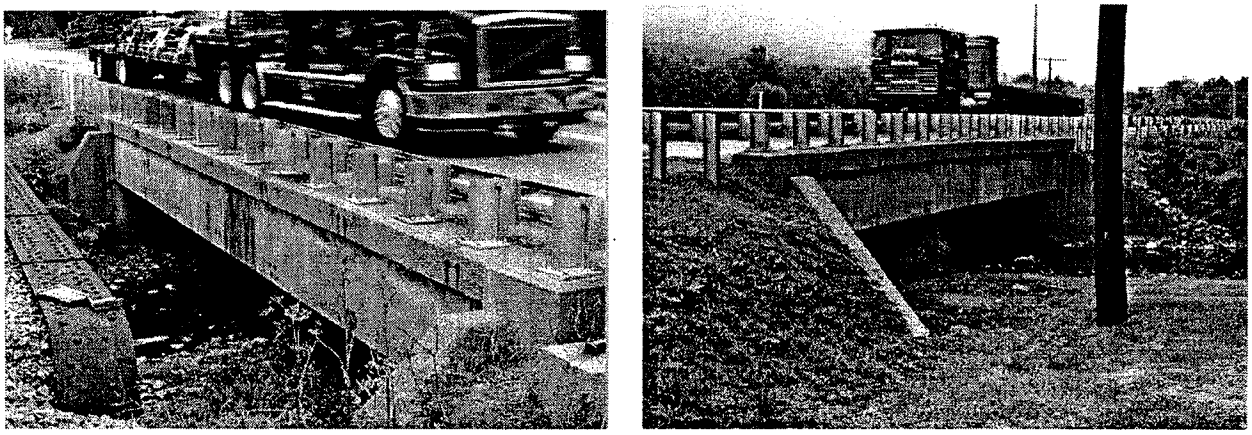

FIGURE 29 East Elevation of Bridge 14-0220-0350-0690 (left) and West Elevation (right).

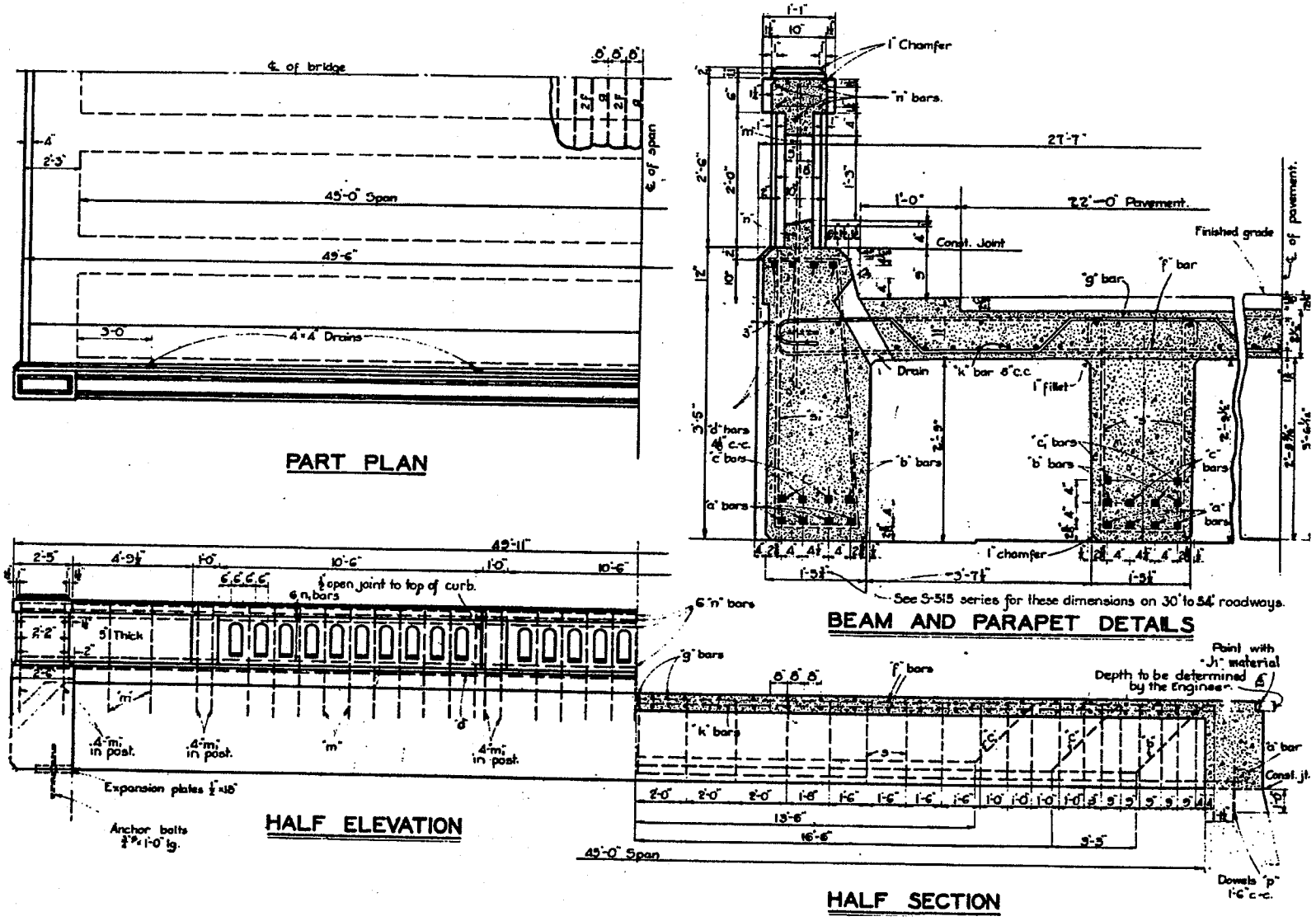

FIGURE 30 Bridge 14-0220-0350-0690 Plans PADOT.

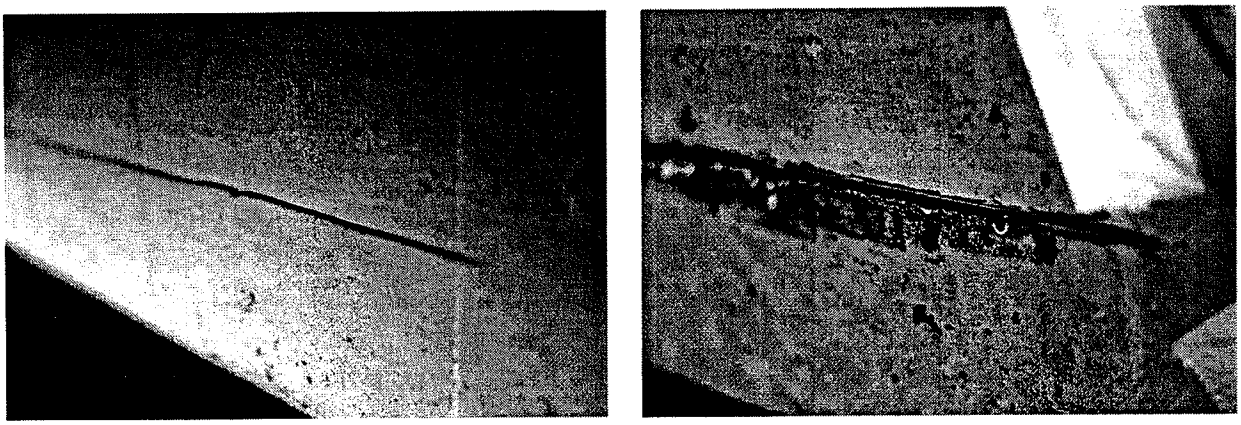

FIGURE 31 Cut Groove for Placement of Optical Sensor (left) and Epoxied Optical Sensor in Place (right).

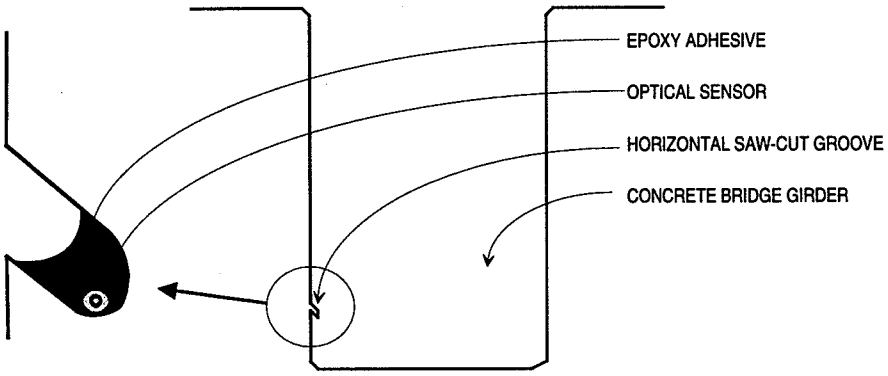

FIGURE 32 Groove Detail for Placement of Optical Sensor.

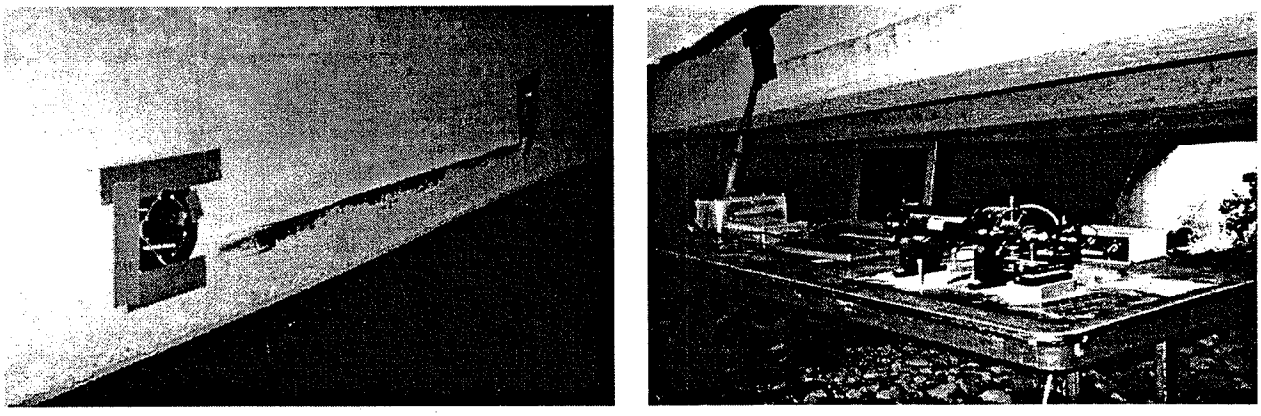

FIGURE 33 Optical Sensor in Place (left) and Field Instrumentation Setup (right).

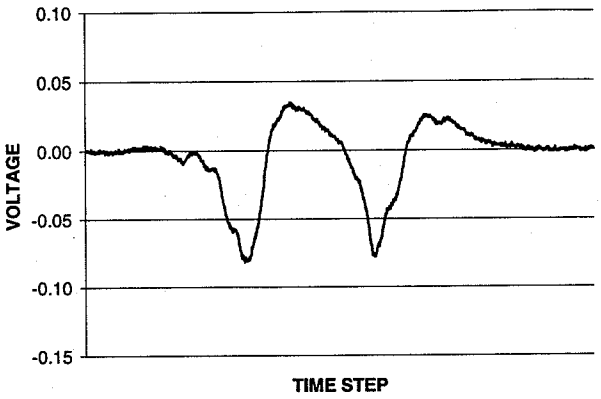

a) Strain Time-History No. 1.

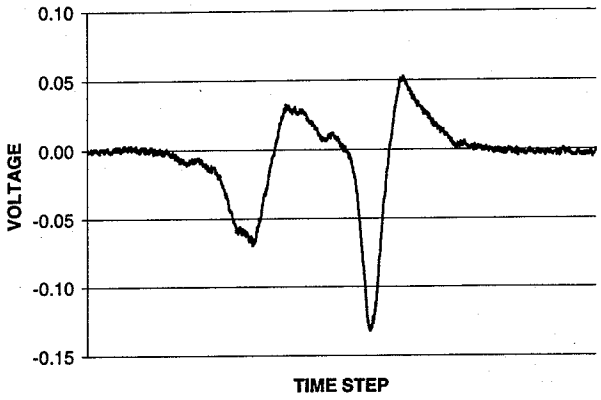

a) Strain Time-History No. 2.

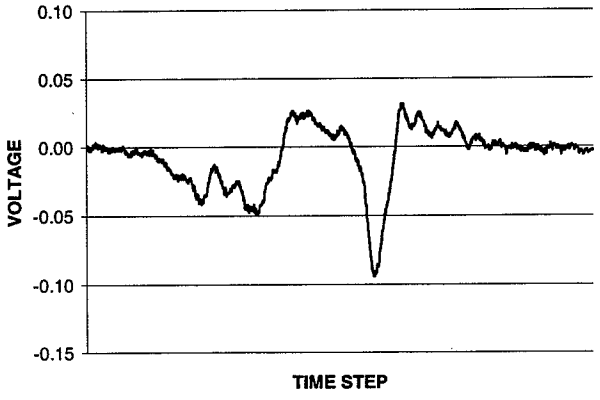

a) Strain Time-History No. 3.

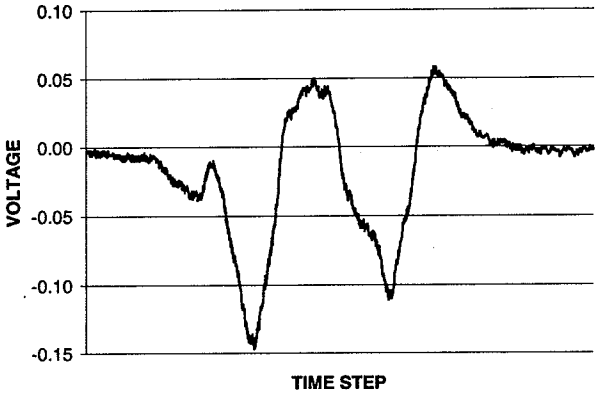

a) Strain Time-History No. 4.

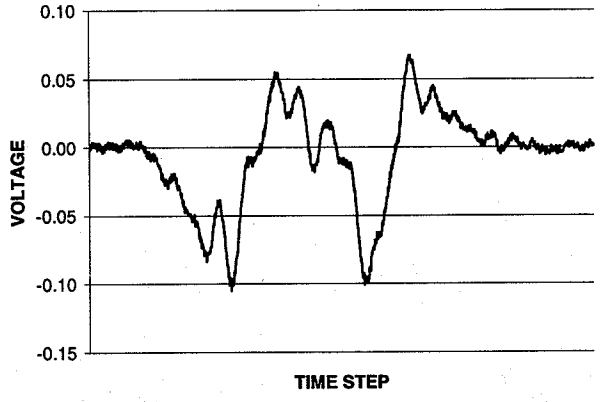

a) Strain Time-History No. 5.

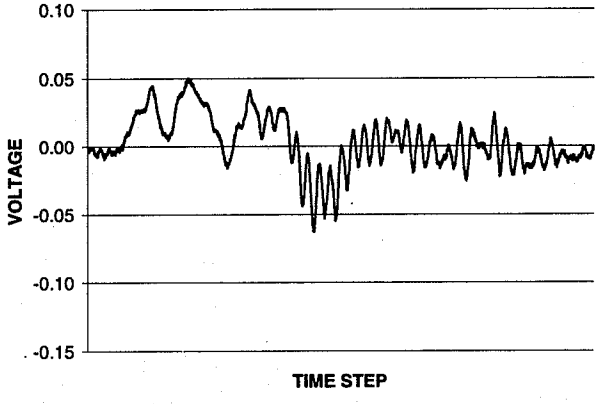

a) Strain Time-History No. 6.

FIGURE 34 Normal Traffic Truck Passage Time-Histories at PADOT Bridge 14-0220-0350-0690 Girder 2.

Several strain time-histories were collected during testing at the bridge site using two optical-fiber sensors. A sample of the time-histories collected is shown in Figure 34. The time-histories represent strain influence lines for various trucks crossing the bridge under normal traffic conditions. The dynamic response of the structure is evident in the time-histories as well as the articulation of the vehicle axles or axle groups.

5.0 CONCLUSIONS

An interferometric optical-fiber sensor has been developed to measure strain in concrete bridge structures. The sensor and corresponding instrumentation for laser light input and output have successfully been demonstrated in the laboratory Phase 2 of the study as well as the field Phase 3 of the study. In addition, a relationship between degree of damage and correlation of FRFs was established that is consistent with past studies. The system requires further development for full deployment in field situations due to the size of the input and output devices and sensitivity of the initiation procedure to focus the input light. These difficulties have been solved in theory, however resources did not permit full development. The major conclusions of the study are as follows:

1. The current state of knowledge for optical-based fiber sensors was researched and presented.
2. An interferometric optical-fiber sensor was developed to measure strain in bridge structures.
3. A preliminary, small, concrete test beam was successfully constructed in the laboratory, demonstrating the sensor attachment, sensor isolation, sensor entrance, and sensor exit techniques to be practical for the larger test structure.
4. The large scale laboratory test structure was successfully constructed with several operating optical sensors embedded.
5. A sensor was successfully retrofitted to the laboratory test structure in anticipation of Phase 3 field applications.
6. The optical sensor performed well under dynamic loads, responding at all frequencies of interest.
7. The optical sensor has promise in reporting damage changes to the structure based on analysis of the FRFs and correlations of the data.
8. The sensor and requisite input, output, and data acquisition system functioned well in the field conditions at the in-service bridge. Strain time-history data was successfully collected for several truck passages under normal traffic.
9. The system is ready for further ruggedization and development for more regular field use.

REFERENCES

Dakin, John, and Brian Culshaw, ed., Optical Fiber Sensors: Principles and Components, Artech House, Boston, 1988.

Fuhr, P. L., D. R. Huston, T. P. Ambrose, and D. M. Snyder, "Stress Monitoring of Concrete Using Embedded Optical Fiber Sensors," Journal of Structural Engineering, ASCE, July 1993, pp. 2263-9.

Huston, D., P. Fuhr, P. Kajenski, and D. Snyder, "Concrete Beam Testing with Optical Fiber Sensors," Nondestructive Testing of Concrete Elements and Structures, ASCE, New York, 1992, pp. 60-9.

Idriss, R. L., and M. B. Kolindouma, "Bridge Monitoring Using an Optical Fibers Sensing System," Building an International Community of Structural Engineers: Proceedings of Structures Congress XIV, ASCE, New York, 1996, pp. 238-44.

Jackson, D. A., "Recent Progress in Monomode Fibre-Optic Sensors," Measurement Science and Technology, May 1994, pp. 621-38.

Kruschwitz, B., R. O. Claus, K. A. Murphy, R. G. May, and M. F. Gunther, "Optical Fiber Sensors for the Quantitative Measurement of Strain in Concrete Structures," First European Conference on Smart Structures and Material, Glasgow, 1992, pp. 241-4.

Maher, M. H., B. Chen, J. D. Prohaska, E. G. Nawy, and E. Snitzer, "Fiber Optic Sensor for Measurement of Strain in Concrete," New Experimental Techniques for Evaluating Concrete Material and Structural Performance, ACI, Detroit, 1994, pp. 1-24.

Masri, S. F., M. S. Agbabian, A. M. Abdel-Ghaffar, M. Higazy, R. O. Claus, and M. J. de Vries, "Experimental Study of Embedded Fiber-Optic Strain Gauges in Concrete Structures," Journal of Engineering Mechanics, ASCE, Aug. 1994, pp. 1696-716.

Measures, R. M., "Advances Toward Fiber Optic Based Smart Structures," Optical Engineering, SPIE, Jan. 1992, pp. 34-47.

Nanni, A., C. C. Yang, K. Pan, J. Wang, and R. R. Michael, Jr., "Fiber-Optic Sensors for Concrete Strain/Stress Measurement," ACI Materials Journal, ACI, May-June 1991, pp. 257-64.

Nawy, E. G., "Use of Fiber Optic Sensors for the Non-Destructive Strength Evaluation and Early Warning of Impending Failure in Structural Components," Research Transformed into Practice: Implementation of NSF Research, ASCE, New York, 1995, pp. 210-20.

Agbabian, M. S., S. F. Masri, M. I. Traini, and O. Waqfi, "Detection of Structural Changes in a Bridge Model," Bridge Evaluation, Repair, and Rehabilitation; Proceedings of the NATO Advanced Research Workshop, A. S. Nowak, ed., Kluwer Academic Publishers, Norwell, Mass., 1900, pp. 133-43.

Biswas, M., A. K. Pandey, and M. M. Samman, "Modal Technology for Damage Detection of Bridges," Bridge Evaluation, Repair, and Rehabilitation; Proceedings of the NATO Advanced Research Workshop, A. S. Nowak, ed., Kluwer Academic Publishers, Norwell, Mass., 1990, pp. 161-74.

Farrar, Charles R., and Scott W. Doebling, Dynamic Characterization and Damage Detection in the I-40 Bridge over the Rio Grande, Los Alamos National Laboratory Report LA-12767-MS, 1994.

Mazurek, D. F., and J. T. DeWolf, "Experimental Study of Bridge Monitoring Technique," Journal of Structural Engineering, ASCE, 116(9), 1990, pp. 2532-49.

Paz, Mario, Structural Dynamics: Theory and Computation, Van Nostrand Reinhold, New York, 1991.

Salawu, O. S., and C. Williams, "Bridge Assessment Using Forced-Vibration Testing," Journal of Structural Engineering, ASCE, 121(2), Feb. 1995, pp. 161-72.

Samman, Mahmod M., and Mrinmay Biswas, "Vibration Testing for Nondestructive Evaluation of Bridges I: Theory," Journal of Structural Engineering, 120(1), Jan. 1994, pp. 269-89.